Bone Micro-Architecture and Physical Activity in Children with Type 1 Diabetes

A Thesis Proposal Submitted to the

College of Graduate and Postdoctoral Studies

in Partial Fulfillment of the Requirements

for the Degree of Master of Science

in the College of Kinesiology

University of Saskatchewan

Saskatoon

By

Anthony Kehrig

Winter 2019

PERMISSION TO USE

In presenting this thesis/dissertation in partial fulfillment of the requirements for a Postgraduate degree from the University of Saskatchewan, I agree that the Libraries of this University may make it freely available for inspection. I further agree that permission for copying of this thesis/dissertation in any manner, in whole or in part, for scholarly purposes may be granted by the professor or professors who supervised my thesis/dissertation work or, in their absence, by the Head of the Department or the Dean of the College in which my thesis work was done. It is understood that any copying or publication or use of this thesis/dissertation or parts thereof for financial gain shall not be allowed without my written permission. It is also understood that due recognition shall be given to me and to the University of Saskatchewan in any scholarly use which may be made of any material in my thesis/dissertation.

Requests for permission to copy or to make other uses of materials in this thesis/dissertation in whole or part should be addressed to:

Dean

College of Graduate and Postdoctoral Studies

University of Saskatchewan

116 Thorvaldson Building, 110 Science Place

Saskatoon, Saskatchewan S7N 5C9

Canada

OR

Dean

College of Kinesiology

University of Saskatchewan

87 Campus Drive

Saskatoon, Saskatchewan S7N 5B2

Canada

ABSTRACT

INTRODUCTION: Individuals with type 1 diabetes (DM1) have a 14-40% greater risk of fractures at all ages. The etiology of greater fracture risk is not known, but possibly related to alterations in bone size, density and micro architecture. Childhood and early adolescent growth years are the best time to optimize the effects of physical activity (PA) on bone development. My primary objective was to compare bone size, density, and micro-architecture at the distal radius and tibia between children with DM1 and typically-developing children (TDC). My secondary objective was to explore the role of daily minutes of moderate-to-vigorous PA (MVPA), vigorous PA (VPA), and daily impacts on bone outcomes that differed between children with DM1 and TDC.

METHODS: Using a cross-sectional design, I analyzed data from 68 children (mean age 11.3, SD 1.9y), categorized into DM1 group (N=21) and TDC group (N=47). High-resolution peripheral quantitative computed tomography (HR-pQCT) measured bone size, density, and micro-architecture at dominant side distal radius and tibia and pQCT measured forearm and lower leg muscle area. Triaxial accelerometers recorded daily minutes of MVPA, VPA, and daily impact counts ≥3.9g. Site-specific MANCOVAs and pairwise comparisons (Bonferroni) assessed group differences (Pillai's trace) and β-coefficients assessed role of PA. Base models were adjusted for sex, maturity, site-specific muscle area, and BMI z-score. Significance set at $p<0.05$.

RESULTS: Bone properties differed between groups at the radius ($F(18,42)=7.59$, $p<0.001$) and tibia ($F(18,42)=2.83$, $p=0.003$). DM1 had lower total area, greater total and cortical densities, greater cortical thickness, lower cortical porosity, pore volume, pore diameter, trabecular area and number, and greater trabecular separation at radius. DM1 had lower cortical porosity, pore volume, pore diameter at tibia. VPA was an independent predictor of cortical pore diameter at the radius (Std. β=-0.18). Significance $p<0.05$.

CONCLUSIONS: Children with DM1 had deficits in total bone size, greater total and cortical densities, and alterations in cortical and trabecular micro-architecture at the radius, as well as alterations in cortical micro-architecture at the tibia. VPA independently predicted cortical pore diameter at the radius.

ACKNOWLEDGEMENTS

I would like to thank Dr. Saija Kontulainen for her knowledge, guidance, and support throughout my postgraduate education. I look forward to continuing to work together in the future. I would also like to thank those in my advisory committee, Dr. Munier Nour and Dr. Nazeem Muhajarine, for taking the time to meet with me throughout this process and for providing me with valuable feedback for my thesis. Thank you to Kelsey Bjorkman, Whitney Duff, and Chantal Kawalilak for collecting anthropometric and bone micro-architecture data from the typically-developing children in my thesis, and many thanks to Yuwen Zheng who collected bone micro-architecture data from the sample of children with type 1 diabetes.

I appreciate all of my participants and their parents who were willing to take the time out of their day to participate in my study. This thesis would not be possible without their involvement. Finally, I would like to thank the Canadian Institutes of Health Research and the Saskatchewan Health Research Foundation for providing us with funding for the Bone Strength Development Study, as well as the Natural Sciences and Engineering Research Council and the Bob and Rita Mirwald Travel Award committee for providing me with funding for tuition and travel expenses throughout my MSc degree.

TABLE OF CONTENTS

LIST OF TABLES

LIST OF FIGURES

LIST OF ABBREVIATIONS

aBMD	Areal bone mineral density, mg/cm^2
AGEs	Advanced glycation end-products
aPHV	Age at peak height velocity, years
Apparent Ct.Th	Apparent cortical thickness, μm
BMD	Bone mineral density, mg/cm^3
BMI	Body mass index, kg/m^2
BV/TV	Trabecular bone volume fraction, %
CDC	Centers for Disease Control and Prevention
Ct.Ar	Cortical area, mm^2
Ct.BMD	Cortical bone mineral density, mg HA/cm^3
Ct.BV	Cortical bone volume, mm^3
Ct.Po	Cortical porosity, %
Ct.Po.Dm	Cortical pore diameter, μm
Ct.Po.V	Cortical pore volume, mm^3
Ct.TMD	Cortical tissue mineral density, mg HA/cm^3
Ct.TV	Cortical total volume, mm^3
CV%RMS	Root-mean squared coefficient of variation, %
DM1	Type 1 diabetes mellitus
DXA	Dual-energy X-ray absorptiometry
Fine Ct.Th	Fine cortical thickness, μm
GRF	Ground Reaction Force, N
HA	Hydroxyapatite

HbA1c	Long-term blood glucose, % glycated hemoglobin
HR-pQCT	High-resolution peripheral quantitative computed tomography
IGF-1	Insulin-like growth factor 1
MANCOVA	Multivariate analysis of covariance
MRI	Magnetic resonance imaging
MVPA	Moderate-to-vigorous physical activity, min/day
PA	Physical activity
pQCT	Peripheral quantitative computed tomography
QUS	Qualitative ultrasound
RCT	Randomized controlled trial
Tb.Ar	Trabecular area, mm^2
Tb.BMD	Trabecular density, mg HA/cm^3
Tb.N	Trabecular number, 1/mm
Tb.Sp	Trabecular separation, μm
Tb.Sp.SD	Trabecular heterogeneity, μm
Tb.Th	Trabecular thickness, μm
TDC	Typically developing children
TMD	Tissue mineral density
Tt.Ar	Total bone area, mm^2
Tt.BMD	Total bone density, mg HA/cm^3
VPA	Vigorous physical activity, min/day

1 INTRODUCTION

Type 1 diabetes mellitus (DM1) is a chronic disease characterized by an insulin deficiency caused by auto-immune pancreatic β-cell destruction (Weber, Haynes, Leonard et al., 2015). Individuals with DM1 also have a 14% greater risk of fractures during childhood and a 40% greater risk of fractures during older age (Weber et al., 2015). The underlying reasons for this greater fracture risk in individuals with DM1 are multifactorial and poorly understood (Weber et al., 2015), but likely related to challenges in bone development, evidenced by a smaller cross-sectional area and lower trabecular bone density at the radius and tibia in children and youth with DM1 (Bechtold, Putzker, Bonfig et al., 2007; Maratova, Soucek, Matyskova et al., 2018; Moyer-Mileur, Dixon, Quick et al., 2004; Roggen, Gies, Vanbesien et al., 2013; Saha, Sievanen, Salo et al., 2009). These findings suggest an unfavourable bone macro-structure for resisting fractures, however much less is known about potential differences in cortical and trabecular bone micro-architecture. Importantly, there is a "window of opportunity" to optimize improvements in bone size when long bone growth accelerates in adolescence (Turner & Robling, 2003). As such, acquiring information of bone micro-architecture in children and youth with DM1 may prove to be of critical importance for identifying underlying skeletal deficits that may contribute to higher fracture rates of individuals with DM1.

Children and adolescents with DM1 have been observed to have lower levels of physical activity (PA) than their typically-developing peers (de Lima, Mascarenhas, Decimo et al., 2017; Michaliszyn & Faulkner, 2010; Valerio, Spagnuolo, Lombardi et al., 2007). Longer daily times spent in moderate-to-vigorous PA (MVPA), vigorous PA (VPA), and a greater number of daily impacts are reported to contribute to the development of a stronger bone structure in typically-developing children (TDC) (Gabel, Macdonald, Nettlefold et al., 2017b; Gabel, Macdonald,

Nettlefold et al., 2017c; Janz, Letuchy, Burns et al., 2014; Kehrig, Bjorkman, Muhajarine et al., 2018); however, the role of PA on bone micro-architecture, particularly cortical bone micro-architecture, has not been assessed in cohorts including children with DM1. This information is necessary to guide the development of PA therapies aimed at optimizing the development of bone size, density, and micro-architecture in children and contributing to a lifelong reduction in rates of bone fractures in both children and youth with DM1 and TDC.

My thesis provides new information of the differences in cortical bone micro-architecture in children and youth with DM1 and explores the independent role of PA on bone size, density, and cortical and trabecular bone micro-architecture in children and youth with DM1 and TDC. This information may further our understanding of what underpins the mechanism of higher fracture risk in children and youth with DM1 and may help to identify PA as a treatment option to reduce lifelong fracture risk in children and youth with DM1 and TDC.

2 LITERATURE REVIEW

In this chapter, I will review the clinical problem of bone fragility in individuals with DM1 and higher fracture rates in children with DM1. I will focus on six key areas: 1. Imaging pediatric bone; 2. Longitudinal changes in children with DM1 and cross-sectional literature assessing bone structure and density in children and youth with DM1; 3. Bone micro-architecture in children and youth, and adults with DM1; 4. Physiological mechanisms underlying bone fragility in individuals with DM1; 5. Theoretical bases of bone adaptation to loading; 6. The role of PA on bone structure and density in TDC and children and youth with DM1.

2.1 Imaging and Assessing Pediatric Bone

Advancements in technology have substantially improved our ability to assess different characteristics of bone. Here, I will provide a critical review of the clinical and research tools commonly used to image or assess bone in children, including dual-energy x-ray absorptiometry (DXA), qualitative ultrasound (QUS), magnetic resonance imaging (MRI), peripheral quantitative computed tomography (pQCT), and high-resolution pQCT (HR-pQCT).

2.1.1 Imaging Pediatric Bone Using DXA

DXA is the standard clinical method for predicting hip and vertebral fracture risk in at-risk populations, such as post-menopausal women (Cummings, Bates, & Black, 2002), and is the standard clinical tool used to measure bone in pediatrics. However, despite the common use of DXA in clinical and research settings, this tool is not ideal for imaging bones in children for several reasons. First, while one of the distinct advantages of DXA is its ability to image the whole body, and sites such as the femoral neck and lumbar spine, this carries with it, a higher radiation exposure than previously mentioned imaging tools (~5mSv for whole-body, hip, and lumbar spine DXA in children) (National Osteoporosis Society, 2004). Second, forearm fractures account for roughly 40% of all pediatric fractures (Mokawem & Scott, 2015), therefore have more clinical relevance than DXA measurements of the total body, the hip, or the lumbar spine. Third, DXA is a planar imaging tool that cannot assess 3D bone structure or true volumetric density values. For this reason, DXA density outcomes are specified as areal (aBMD), instead of volumetric (vBMD) (Bolotin & Sievanen, 2001). This is especially a problem in children, as DXA-derived aBMD is influenced by bone size and is artificially higher in individuals with larger bones (Kontulainen, Kawalilak, Johnston et al., 2013). Lastly, DXA unavoidably attributes

±20% of the error in aBMD to differences in beam absorption characteristics of other tissues such as fat, muscle, and marrow surrounding or inside bone (Bolotin & Sievanen, 2001).

2.1.2 Imaging Pediatric Bone Using QUS and MRI

QUS is safe (no radiation), portable, easy to use, and can be used to assess bones at common fracture regions at the wrist, making this an attractive tool for researchers assessing bone in a pediatric population (Baroncelli, 2008). Despite these advantages, there is a general scepticism of findings from studies using QUS to assess bone. First, QUS cannot directly measure BMD, instead it measures the speed of sound (SOS) through bone tissue, which is used as a surrogate measurement of bone mineral quality. Second, this tool is limited by using different variables to estimate bone mineral quality across a large variety of QUS devices (Baroncelli, 2008), therefore limiting the external validity of QUS findings to particular devices. Third, there is still a poor level of knowledge on the physical mechanisms surrounding QUS measurement of bone (Baroncelli, 2008). This is further complicated by different levels of bone mineralization in pediatric bone tissue affecting QUS outcomes designed to measure fully mineralized bone. Lastly, QUS is not an imaging tool so it cannot be used to assess bone structure, and there is difficulty comparing these results to x-ray based densitometric techniques (Baroncelli, 2008).

Similar to ultrasound, MRI uses no radiation. Instead, MRI maps the location of hydrogen atoms in the body, mostly present in water and fat in the body, and uses this information to measure contrasts in tissue properties (Majumdar, Genant, Grampp et al., 1997). For this reason, MRI is most applicable for measuring properties of soft tissue, and less commonly, bone. However, MRI can still be used to capture 3D-images of bone and assess trabecular bone micro-structure (Chen, Shepherd, McMillan et al., 2019; Majumdar et al., 1997). However, inherent limitations of MRI do not allow researchers the ability to use this tool to

assess cortical bone micro-architecture (Majumdar et al., 1997). This is a notable limitation as no previous studies have assessed cortical micro-architecture in children with DM1, which may be a critical determinant of bone strength, as previous studies have found that cortical thickness, measured using pQCT, predicts 72% of the variance in bone failure load based on mechanical testing at the radius shaft (Muller, Mitton, Moilanen et al., 2008).

2.1.3 Imaging Pediatric Bone Using pQCT, and HR-pQCT

pQCT is another common tool used to measure volumetric BMD, 3D bone macro-structure and estimate bone strength at distal and shaft sites at the radius and tibia (200-800μm voxel size) (Figure 1). One of the benefits of this low radiation dose tool is that it offers another important application for its use musculoskeletal research, by being able to measure muscle area at the forearm and lower leg (Björkman, Duff, Frank-Wilson et al., 2017). As with most x-ray-based imaging techniques, pQCT scans are susceptible to motion artefacts. This can prove challenging in pediatric populations as children must stay relatively motionless for several minutes during scans.

Figure 1. Peripheral computed tomography (pQCT) scans at distal and shaft sites of the radius and tibia.

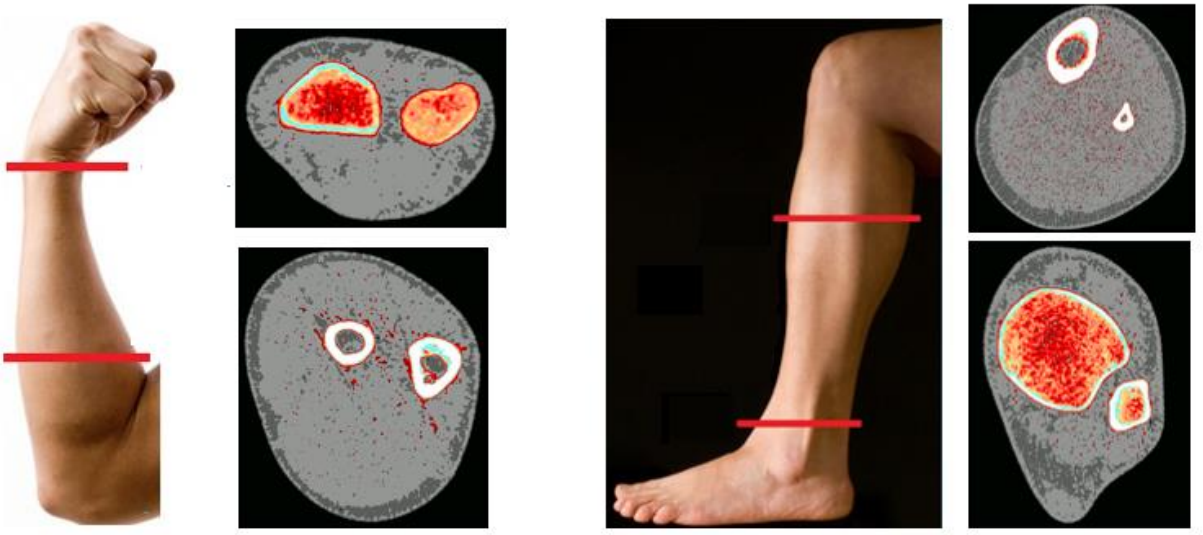

With further technological advancements, came improvements in imaging resolutions and the ability to assess bone micro-architecture using QCT. The higher resolution of the HR-pQCT (82μm voxel size) allows researchers to assess both cortical and trabecular micro-architecture after separating cortical and trabecular bone compartments (Figure 2) (Kawalilak, Bunyamin, Bjorkman et al., 2017). HR-pQCT has also been validated for its use in adults against gold standard measurements of bone micro-architecture (micro-CT) in cadavers (Boyd, 2008; Laib & Ruegsegger, 1999). However, there are still several limitations of using HR-pQCT to assess bone micro-architecture in children. First, the accuracy of this tool has not been validated against micro-CT in a child population, as this would require micro-CT imaging of bone samples obtained from child cadavers. However, the measurement error in children has been recently determined in our lab (Bunyamin, Bjorkman, Kawalilak et al., 2019). Second, the 82μm voxel size is very close to the low end of trabecular thicknesses at the distal tibia (D. Liu, Burrows, Egeli et al., 2010) and would only be able to capture larger cortical pores >82μm in adults (Patsch, Burghardt, Kazakia et al., 2011). These structures are even smaller in children, and it follows that researchers may need to develop a tool with an even higher resolution for pediatric bone assessment. There has been recent progress in improving the spatial resolution of this tool, as the manufacturers of the Xtreme CT have recently developed a second generation of this tool (Xtreme CT II) capable of measuring bone using a 60μm voxel size, however despite improvements in spatial resolution, large voxel size remains a limitation in imaging smaller structures in bone. Third, while certain micro-architectural outcomes such as trabecular number are truly 3D and derived from distance transformations – determined by the average diameter of spheres between trabecular ridges, other outcomes such as trabecular thickness and separation, rely on assumptions of the underlying bone structure (Burrows, Liu, Moore et al., 2010; X. S.

Liu, Zhang, Sekhon et al., 2010) and were validated in an adult population. However, indirect measurement of bone micro-architectural outcomes are not unique to HR-pQCT, as similar methods are used to derive trabecular micro-architecture outcomes using micro-MRI (Majumdar et al., 1997). HR-pQCT is widely considered an excellent, and clinically-relevant tool for measuring bone characteristics relevant to bone fractures, as evident from a recent prospective study that found that cortical and trabecular micro-architecture outcomes were associated with fracture risk in older men and women, independent of DXA-measured aBMD (Samelson, Broe, Xu et al., 2019). Whereas in children, there is evidence of associations between HR-pQCT bone outcomes and low-energy fractures in boys and girls (Määttä, Macdonald, Mulpuri et al., 2015; Macdonald, Maatta, Gabel et al., 2018). However, as HR-pQCT was designed and validated for use in adults, we must remain cautious in our interpretation of these findings in children and youth.

Figure 2. High-resolution peripheral computed tomography (HR-pQCT) scan illustrating the separation of cortical bone (blue) and trabecular bone (green), and the cortical porosity (grey) at the distal tibia.

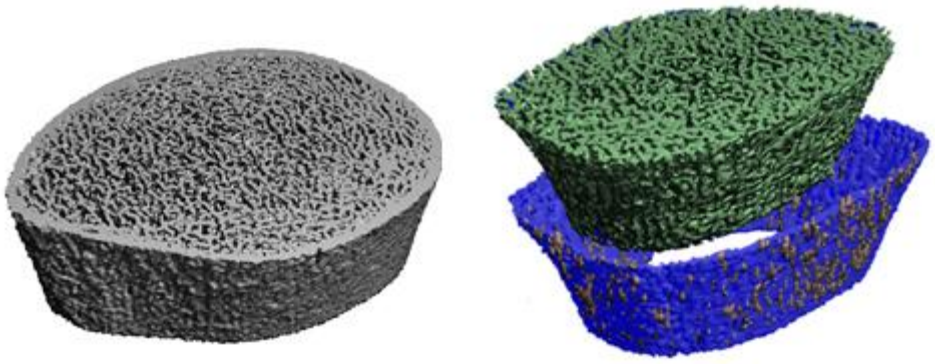

2.2 Bone Macro-Structure and Density in Children and Youth with DM1

2.2.1 Longitudinal Changes in Children with DM1 Compared to Predicted Changes in a TDC Reference Population

Findings from two studies using pQCT to measure bone macro-structure and density report deficits in cortical bone area, density, and thickness, as well as trabecular bone area, content, and density in children with DM1 (Table 1). One of these studies reported skeletal deficits in a group of children with DM1 compared to normative data, z-scores, and predicted changes in TDC at distal and shaft sites at the radius using pQCT (Bechtold et al., 2007), while the other study reported deficits in a group of children with DM1 compared against predicted annual changes of a regional reference population at distal and shaft sites at the tibia using pQCT (Moyer-Mileur et al., 2004). When compared to reference data, baseline measurements of children (mean age=9.9y) suggested that children with DM1 had a lower trabecular density at the distal radius and a lower total and cortical cross-sectional area, and cortical BMD at the radius shaft (Bechtold et al., 2007). It is important to note that these differences normalized and were not longer present after 5.5 years (mean age=15.4y). Moyer-Mileur et al. (2004) found similar deficits in bone size outcomes at the distal tibia, as well as an 8.6% lower torsional bone strength in children with DM1. Adolescents in the DM1 group had a lower cortical area (-7.6%), cortical content (-6.9%), cortical thickness (-4.9%), trabecular area (-5.1%), trabecular content (-10.9%), and trabecular density (-5.9%) at baseline and similar deficits at the 12-month follow-up (Moyer-Mileur et al., 2004). After 12 months, there were increases in cortical bone properties in both groups; however, increases in bone area, content, density, and estimated torsional bone strength were lower in the DM1 group (Moyer-Mileur et al., 2004).

2.2.2 Cross-Sectional Evidence

Cross-sectional studies reported similar deficits in total and trabecular bone size and densities, as well as lower cortical areas and thicknesses, and greater cortical densities (Table 1). Maratova et al. (2018) reported that children with DM1 had a greater cortical density, along with a lower trabecular density, cortical thickness, and torsional bone strength at the tibia. There were no significant differences in total and cortical cross-sectional bone area between children with DM1 and TDC (Maratova et al., 2018). Other researchers have suggested that DM1 is associated with a smaller cortical area in boys at the radius (-12% lower in boys) and in boys and girls at the tibia (-4% lower in girls and -9% lower in boys), and a lower trabecular density (-4% girls, -5% boys) at the distal tibia (Saha et al., 2009). They also reported that children with DM1 had a lower torsional bone strength at the radius (-5% girls, -17% boys) and tibia shaft (-7% girls, 12% boys) compared to TDC (Saha et al., 2009). Roggen et al. (2013) investigated differences between older adolescents and young adults with DM1. They reported a lower total cross-sectional area at the radius in males (-5.6%) and females (-15.6%), but no differences in trabecular density at the radius (Roggen et al., 2013). Other cross-sectional studies report similar findings of lower trabecular bone density in boys and girls with DM1 (Heap, Murray, Miller et al., 2004; Lettgen, Hauffa, Mohlmann et al., 1995). Both studies reported a lower trabecular bone density in adolescents (-3.8%) (Heap et al., 2004) and children (-18.9%) with DM1 (Lettgen et al., 1995). Findings using digitalized X-rays at the second metacarpal support previous findings of smaller, and weaker bones children with DM1 (Franceschi, Longhi, Cauvin et al., 2017), however these findings are based on measurements obtained using planar imaging tools, which do not offer the same clinical importance as the distal radius (common fracture site) and tibia (weight-bearing site).

2.3 Bone Micro-Architecture in DM1

2.3.1 Bone Micro-Architecture in Children and Youth with DM1

There is no evidence of differences in cortical micro-architecture and limited evidence of differences in trabecular micro-architecture between children and youth with DM1 and TDC (Table 1). Findings from one study using MRI to measure bone micro-architecture, reported that children with DM1 have a lower trabecular volume, trabecular number, and higher trabecular separation than their typically-developing peers (Chen et al., 2019). However, MRI is unable to assess cortical bone micro-architecture, which is a crucial determinant of overall bone strength (Muller et al., 2008; Nishiyama, Macdonald, Moore et al., 2012). No studies have assessed cortical bone micro-architecture in children and youth with DM1, as this measurement requires HR-pQCT. Obtaining HR-pQCT scans in children with DM1 would provide new evidence of cortical bone micro-architecture and add to current evidence of deficits in trabecular micro-architecture in children and youth with DM1, which may help us to reveal the origins of bone fragility in childhood.

2.3.2 Bone Micro-Architecture in Adults with DM1

Evidence of differences in bone size, density, and cortical and trabecular micro-architecture as measured by HR-pQCT are only reported in adults with DM1 (Shanbhogue, Hansen, Frost et al., 2015). They found that adults with DM1 and the presence of microvascular disease had deficits in total BMD (-10%, -17%), trabecular BMD (-18%, -20%), trabecular thickness (-12%, -14%), bone stiffness (-14%, -16%), and failure load (-14%, -15%) at the distal radius and tibia, respectively; and additional deficits in cortical area (-15%), trabecular bone-volume ratio (-20%), as well as a greater trabecular separation (+12%) and heterogeneity (+19%) at the distal tibia compared to adults with DM1 and no presence of microvascular disease (Shanbhogue et al.,

2015). Independent of the presence of microvascular disease, all adults with DM1 had a larger total area (+13%) and trabecular area (+18%), as well as a lower total density (-11%), cortical density (–3%), and cortical thickness (–8%) at the distal radius compared to adults without DM1. They reported no differences between the DM1 and control group at the distal tibia (Shanbhogue et al., 2015).

2.4 Physiological Mechanisms Underlying Bone Fragility in Individuals with DM1

It is important to discuss the physiological mechanisms underlying bone fragility in DM1, as evidence has suggested it is a condition of low bone turnover (Hygum, Starup-Linde, Harslof et al., 2017; Napoli, Chandran, Pierroz et al., 2017). The mechanisms underlying bone fragility in DM1 are complex and may be related to hyperglycaemia, oxidative stress and the accumulation of advanced glycation end-products (AGEs) that compromise collagen properties, increased marrow adiposity, release of inflammatory factors and adipokines from visceral fat (Napoli et al., 2017). Most of the recent studies assessed in a systematic review have indicated lower levels of bone turnover markers, and a lower activation frequency of bone remodelling units in adults with DM1 (Hygum et al., 2017). Smaller cross-sectional bone areas at the radius or tibia show associations with poor glycemic control (↑ HbA1c), lower IGF-1, insulin, lower levels of vitamin D (Napoli et al., 2017). Glycemic control may prove to be a factor influencing bone fragility, as there was a higher degree of trabecular bone mineralization in iliac crest bone biopsies of fracturing adults with DM1 compared to non-fracturing adults with DM1. They also found that the degree of non-enzymatic collagen cross-linking was higher in fracturing adults with DM1 compared to adults without DM1 (Farlay, Armas, Gineyts et al., 2016). Degree of trabecular mineralization and non-enzymatic cross-linking were also both positively correlated with higher

HbA1c levels (i.e. higher bone mineralization and lower bone turnover state) (Farlay et al., 2016). They suggest that excess glucose in the blood contributes to a higher bone mineralization rate and the lower remodelling rate allows bone to be further mineralized before being replaced, resulting in a less flexible; and more rigid bone matrix, susceptible to low-energy fractures (Farlay et al., 2016).

2.5 Bone Structure Adaptation to Loading Daily Physical Activity and Impacts and Bone Structure

2.5.1 Theoretical Bases of Bone Adaptation to Loading

The underlying principle highlighting the influence of mechanical loading on bone adaptation is known as the mechanostat hypothesis (Frost, 1987). According to the mechanostat hypothesis, bone modeling and remodelling processes are guided by mechanisms sensing the elastic deformation of bone (Frost, 1987). These bone adaptations are site-specific and as the result of loads generated both internally, through muscle forces; and externally, through external reaction forces such as impacts (Schoenau & Frost, 2002). It is important to note that the mechanical loads applied to bone are different than bone strain; however, they are interconnected. Mechanical loads induce stress on load-bearing bones, thereby causing a material strain on bone tissue (Al Nazer, Lanovaz, Kawalilak et al., 2012). Bone strain is the governing stimuli for the bone remodelling process and can be defined as the deformation of bone through the relative displacement of the particles that make-up bone (Al Nazer et al., 2012). Osteocytes can sense bone strain and guide bone adaptation through cell signalling. These signals are sent to other bone cells; namely osteoblasts and osteoclasts, to begin the bone remodelling process through bone formation and bone resorption (Binkley, Berry, & Specker, 2008). During skeletal

development, bone modelling occurs which allows bone to grow in length, and in width, through the formation of new bone on the outer surface (Binkley et al., 2008). The degree of bone modelling is in part, determined by genetics, but also by the strains that bone is exposed to (Binkley et al., 2008). This presents us with a window of opportunity during peak bone growth in which we may use PA to optimize adaptations of bone that carry into adulthood (Turner & Robling, 2003).

2.5.2 Using Accelerometers to Estimate Bone Loading in Children and Youth

Using wearable accelerometers, we are able to record daily minutes of MVPA and VPA (Kehrig, Bjorkman, Muhajarine et al., 2019; Trost, Loprinzi, Moore et al., 2011) and daily number of impacts in children and youth (Kehrig et al., 2019). It is not possible to measure principle bone strains directly, as the axes of the forces causing this strain are not known and change with different movements (Al Nazer et al., 2012). A close approximation to this would require multiple strain gauges to be fitted to different regions of exposed bone directly in line with the forces being generated (Al Nazer et al., 2012), which is not realistic for child populations. However, it is possible to measure the mechanical bone loading causing bone strain by measuring ground reaction forces (GRF) in children (Meyer, Ernst, Schott et al., 2015). A distinct drawback to this method is that you can only able to obtain a "snapshot" of the GRF using force plates, which does not allow researchers to estimate daily average levels of bone loading. Instead, accelerometers may be used to record daily levels of PA as an estimate of bone loading (Meyer et al., 2015). Accelerometer activity counts were originally validated against estimates of VO^2 max in children (Evenson, Catellier, Gill et al., 2008; Trost et al., 2011), however, they are correlated with mechanical loading, as measured by GRF in children. Activity counts and raw acceleration (resultant vector) values from hip-worn accelerometers are

correlated to mean GRF (r=0.90) in ActiGraph GT3X accelerometers in children, however it is important to note that the accelerometers used in this study consistently overestimated GRF (Meyer et al., 2015).

2.5.3 MVPA, VPA, and Impacts and Bone Size, Density, and Micro-Architecture in Children and Youth

Previous research indicates a beneficial relationship between MVPA, VPA, and impacts, and trabecular and cortical micro-architecture in TDC, but evidence of these relationships in children and youth with DM1 is limited. Longitudinal findings from Gabel et al. (2017c) reported that MVPA positively predicted trabecular bone volume fraction and failure load at the radius, as well as total area, cortical porosity, trabecular bone volume fraction, and estimated bone failure load at the tibia (Gabel et al., 2017c). Gabel et al. (2017b) also reported that the volume and frequency of VPA was positively associated with bone failure load at the tibia. Children in the upper quartile of VPA bout frequency had a greater bone failure load (+10%) at the tibia across adolescent years than children in the lowest quartile of VPA bout frequency (Gabel et al., 2017b). Results from my previous work also provided evidence of the benefits of MVPA and VPA in TDC. We reported that average daily minutes of MVPA and VPA independently predicted the variance in bone strength at the tibia, but not at the radius (Kehrig et al., 2019). Our findings also showed that impact counts greater than or equal to 3.9g (1g = 9.81 m/s^2) exhibited a positive relationship with tibia bone strength in TDC (Kehrig et al., 2019)

There is no evidence of a relationship between objectively-measured PA and cortical and trabecular micro-architecture in children and youth with DM1 in previous literature. However, an RCT investigating the role of exercise on DXA-measured aBMD in children with DM1 found a similar magnitude of improvement in total body aBMD, and lumbar spine aBMD for children

with DM1 and TDC (Maggio, Rizzoli, Marchand et al., 2012). Their results suggest that there was no difference in bone adaptation to PA in children and youth with DM1 (Maggio et al., 2012).

2.5.4 Mechanical Loading Adaptations in a DM1 Animal Model

Evidence from DM1 mouse models have suggested that hyperglycemia may lead to impairments in bone's adaption to mechanical loading (Parajuli, Liu, Li et al., 2015). They observed positive differences in cortical bone area (+14%, +16%, +6.5%) and cortical bone thickness (11%, +10%, +6.5%) between the loaded and non-loaded ulna assessed using bone histomorphometry in male and female wild-type mice (control models) and female Akita mice (mild diabetes model). Whereas, male Akita mice (severe diabetes model) saw no differences between their loaded and non-loaded ulna (Parajuli et al., 2015). It is important to note that findings from mature animal models may not reflect adaptations in immature human bone. Instead, these findings warrant further investigation of the role of PA and bone characteristics in diabetic populations.

Table 1. Previous literature reporting differences between children and youth with type 1 diabetes (DM1) and typically developing children and youth (TDC).

First Author	Year	Study Design	Participants	Bone Imaging	Results
Bechtold	2007	DM1 5.5-year change compared to predicted changes of TDC reference population	41 boys and girls (mean 9.87, SD 2.3y) with DM1	pQCT at distal and shaft sites of radius	At baseline, distal site, trabecular density was higher in DM1 than in TDC, irrespective of age, sex, and Tanner stage. At the shaft, DM1 had significantly reduced total, cortical, and medullary area as well as cortical density at first measurement After 5.5 years, these parameters had normalized. SSI and muscle area were not different from reference population at the first and second measurements
Chen	2019	Cross-sectional	32 children (mean 13.7y) with DM1 and 26 controls (13.8y)	DXA and MRI at proximal end of tibia	DM1 had lower trabecular volume, trabecular number, and higher trabecular separation than controls Bone formation (assessed by bone-specific alkaline phosphatase) was lower in children with poorer glycemic control
Franceschi	2017	Cross-sectional	96 boys and girls (mean 10.5, SD 3.1y) with DM1	Digitalized X-rays at 2nd metacarpal and QUS at distal phalanges	Outer diameter, inner diameter, cortical area, and medullary area were smaller in DM1 than in controls. BBRI (an index of bone strength) was lower compared to the normal values. Speed of sound (SOS) was higher in DM1, while bone transmission time (BTT) was not different Inner diameter and medullary area were smaller in Low HbA1c compared to High HbA1c, but not in outer diameter, cortical area, metacarpal index, and BBRI. No difference between Low HbA1c and High HbA1c was found for SOS or BTT

Heap	2004	Cross-sectional	55 adolescents (12 to 17y) with DM1 and 95 TDC	DXA and pQCT at distal and shaft sites of tibia	DM1 group had lower trabecular density at the tibia (-3.8%) compared to controls. Lower femoral neck aBMD (-7.8%) and BMAD (-7.3%), and whole-body BMC (-6.9%), aBMD (-4.9%), BMAD (-3.4%), and whole-body BMC in relation to height (-6.2%) or lean mass (-8.8%) compared to controls There were no differences in cortical area, content, or density
Lettgen	1995	Cross-sectional	21 children and adolescents with DM1 and age- and sex-matched controls	pQCT	DM1 group had lower trabecular bone density (-18.9%), while total bone density and cortical bone density were not significantly lower
Maggio	2010	Cross-sectional	27 children with DM1 and 32 controls (mean 10.5, SD 2.5y)	DXA	aBMD results were similar among DM1 and healthy subjects. Proportion of children with low aBMD was identical in both groups
Maggio	2012	RCT (4 groups; DM1 and TDC; exercise and control groups)	27 children with DM1 and 32 controls (mean 10.5, SD 2.5y)	DXA	The intervention had a moderate to large effect on LBM but not on other anthropometry variables. TB and LS2–LS4 aBMD changes were higher in both intervention groups. Changes during the exercise intervention were not different between DM1 and TDC groups or sexes
Maratova	2018	Cross-sectional	95 adolescents (mean 16.2, SD 1.2y) with DM1	pQCT at distal and shaft sites of tibia	DM1 had greater cortical density and lower cortical thickness, trabecular density, and SSI compared to the reference. Total and cortical bone areas at the tibia shaft were not different between DM1 and the reference

Moyer-Mileur	2004	DM1 12-month change compared to predicted changes in TDC reference population	42 children with DM1 and 199 controls (12 to 18y)	DXA and pQCT at distal and shaft sites of tibia	At baseline, DM1 had lower tibia cortical area (-7.6%), content (-6.9%), and thickness (-4.9%), trabecular area (-5.1%), content (-10.9%), and density (-5.9%), SSI (-8.6%), lumbar spine BA (-6.6%), BMC (-11.9%), aBMD (-4.9%), BMAD (-1.3%), and whole body BA (-2.1%), and BMC (-8.3%). DM1 had slightly higher cortical density (0.8%), but difference disappeared at 12 months After 12 months, tibia cortical bone characteristics increased in both groups; however, lower gains for cortical area, content, density, and SSI were observed in subjects with DM1. Tibia trabecular bone values remained constant in both groups.
Roggen	2013	Cross-sectional	56 adolescents and young adults with DM1 (females 18.1y and males 17.9y) and 47 healthy controls (females 18.8y and males 19.1y)	pQCT at distal radius	Male and female DM1 patients had a smaller total radius area (-5.6%, and -15.6%, respectively). Similar radius trabecular density between DM1 and control groups

Saha	2009	Cross-sectional	48 adolescents with DM1 (females 15.1y and males 15.2y) and controls (females 15.5y and males 15.9)	DXA and pQCT at distal and shaft sites of radius and tibia	No difference between DM1 and TDC at distal radius At radius shaft, DM1 group had lower total bone content, cortical area, cortical content, and SSIp. At distal tibia, DM1 group had lower total bone area, content, cortical area, and trabecular density. At tibia shaft, DM1 group had lower total bone content, cortical area, and SSIp BMC 2-14% lower in DM1 group at all skeletal sites, including the proximal femur and lumbar spine Among diabetic boys, the mean deficit in BMC calculated from all measured skeletal sites was more than 10%, while among the girls it was less than 5%. Diabetes-associated deficit seemed to affect boys more than girls
Weber	2019	Prospective cohort study (baseline diagnosis and 1-year follow-up)	36 children with DM1 (mean 14.2y)	DXA and pQCT at distal and shaft sites of tibia	All children with DM1 had a lower cortical bone density compared to a TDC reference population. Both good and bad glycemic control groups had lower trabecular density

Abbreviations: aBMD = areal bone mineral density, BA = bone area, BBRI = bending breaking resistance index, BMAD = bone mineral apparent density, BMC = bone mineral content, BTT = bone transmission time, LS = lumbar spine, QUS = qualitative ultrasound, SD = standard deviation, SOS = speed of sound, SSI = stress-strain index, TB = total body, vBMD = volumetric bone mineral density.

3 OBJECTIVES AND HYPOTHESES

3.1 Research Objectives

3.1.1 Primary Research Objective

The primary objective of my thesis was to compare bone size, density, and cortical and trabecular micro-architecture at the distal radius and tibia between children with DM1 and TDC after adjusting for covariates.

3.1.2 Secondary Research Objective

The secondary objective of my thesis was to explore the role of daily minutes of MVPA, VPA, and daily impacts on bone outcomes that differed between children with DM1 and TDC.

3.2 Hypotheses

3.2.1 Hypothesis for Primary Research Objective

For my primary objective, I hypothesized there will be differences in bone size, density, and cortical and trabecular micro-architecture at the distal radius and tibia between children with DM1 and TDC.

3.2.2 Hypothesis for Secondary Research Objective

For my secondary objective, I hypothesized daily minutes of MVPA, VPA, and daily impacts will independently predict bone outcomes that differed between children with DM1 and TDC.

4 METHODS

4.1 Study Design and Participants

I used a cross-sectional study design. I assessed data from 21 children with DM1 (12 girls, mean age 12.1, SD 2.1y) and 47 TDC (22 girls, 10.9, 1.6y) (Figure 3). We recruited 38 children with DM1 from LiveWell diabetes clinics, the D-camp at Christopher Lake, SK, and diabetes family days in Saskatoon and Regina, SK. In addition, I had access to previously collected data from a cohort of 170 TDC recruited from schools and community programs in Saskatoon, Canada (Bunyamin et al., 2019). To be included in my thesis analyses, participants had to have valid HR-pQCT data at the radius or tibia, a valid triaxial accelerometer recording of physical activity and impact counts, and valid pQCT data at the forearm or lower leg. I will provide a detailed definition of how I determined the validity of my data for each of these tools later in this chapter. We also obtained informed assent from our participants and consent from their parents or guardians. This study was approved by the University of Saskatchewan Biomedical Research Ethics Board.

Figure 3. Participant inclusion flowchart.

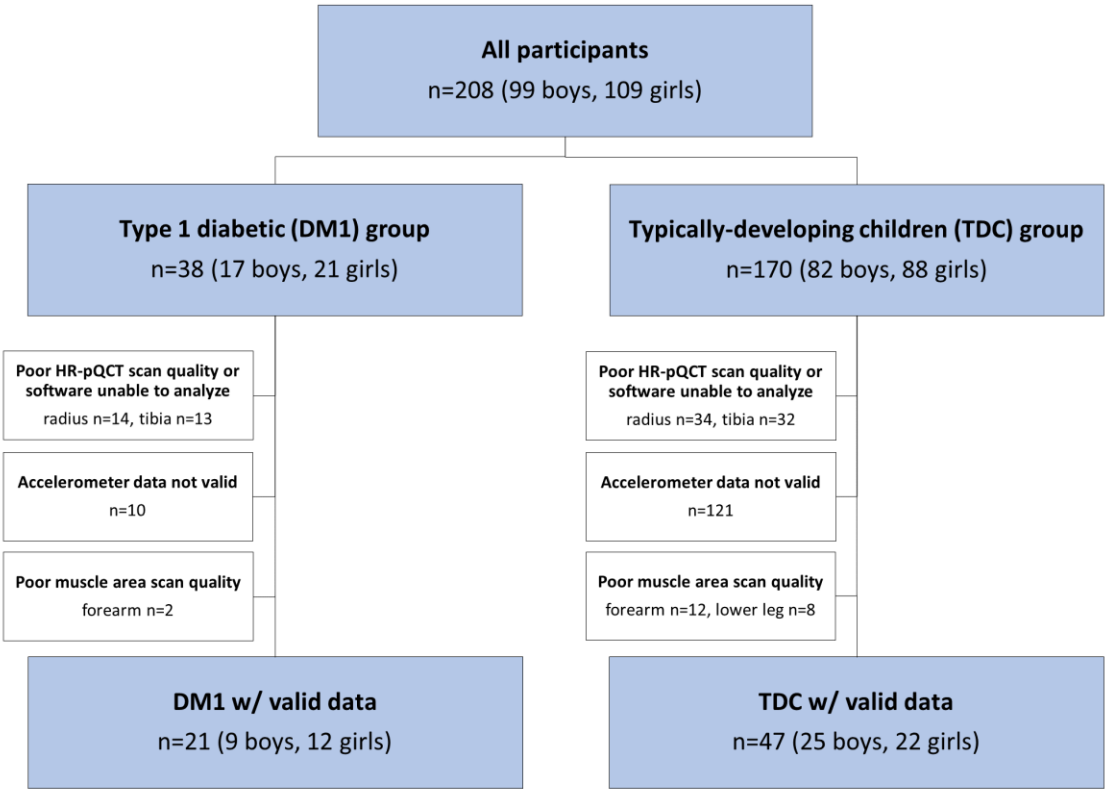

4.2 Anthropometrics, Nutrition and Other Background Characteristics

We measured anthropometric variables such as height, sitting height, body mass, ulna and tibia lengths following previously described methodology (Duff, Björkman, Kawalilak et al., 2017). I measured height, sitting height, and limb lengths three times and used the median value in my analyses. Maturity was assessed by estimating the years from age at peak height velocity (aPHV) for each participant using sex-specific equations (Moore, McKay, Macdonald et al., 2015). Estimating somatic maturity allowed me to account for differences in maturation timepoints of boys and girls (Gabel, Macdonald, & McKay, 2017a). Body mass indexes (BMI, kg/m^2), BMI z-scores, and BMI percentile ranks were calculated for each child in the study using the Children's

BMI Group Calculator available on the Centers for Disease Control and Prevention (CDC) website. Reference data for this tool was obtained from CDC growth charts from the year 2000 (Kuczmarski, Ogden, Grummer-Strawn et al., 2000). BMI z-scores are commonly used in child populations as a measure of relative body size adjusting for the age and sex. Another technician and I assessed daily average dietary protein (g/day), calcium intake (mg/day), and vitamin D intake (IU/day) using self-reported data collected from a food-frequency questionnaire (Block 98, Nutrition Quest). The validity and reliability of this questionnaire has been previously assessed in adults (Boucher, Cotterchio, Kreiger et al., 2006). I also obtained age at DM1 diagnosis (years), years since DM1 diagnosis (years), and averaged long-term blood glucose levels (HbA1c, %) of each child from electronic medical records after receiving approval from the Saskatchewan Health Authority.

4.3 Bone Size, Density, and Cortical and Trabecular Micro-Architecture

Two trained technicians obtained scans at the dominant distal radius (7% ulna length) and tibia (8% length) using HR-pQCT (Xtreme CT) and followed our validated protocols (Bunyamin et al., 2019; Kawalilak et al., 2017). If motion artefacts were present, the technician took a second scan at the same site. Each image was graded based on a 5-point scale defined by the manufacturer (Pialat, Burghardt, Sode et al., 2012). Scans graded 4 or 5 or scans that the software was unable to analyze (both mainly due to excessive patient movement), were determined to be invalid and excluded from analyses. We used the manufacturer's software to trace the outer boundary of the bone and manually corrected any errors in the tracing that did not match the outer bone boundary to obtain standard evaluation outcomes. Standard evaluation outcomes include: trabecular area (Tb.A, mm^2), total and trabecular bone density (Tt.BMD and

Tb.BMD, mg HA/cm^3), trabecular bone volume fraction (BV/TV, %) (the ratio of trabecular bone volume to total bone volume in the region of interest), trabecular number (Tb.N, 1/mm), trabecular thickness (Tb.Th, μm), trabecular separation (Tb.Sp, μm), and trabecular heterogeneity (Tb.Sp.SD, μm).

Another trained technician and I then used an automated segmentation algorithm to trace an inner cortical boundary between the cortical and trabecular bone compartments, and manually corrected any errors in the tracing, to separate the cortical bone region before analyzing scans with advanced cortical analysis (Burghardt, Issever, Schwartz et al., 2010). Advanced cortical analysis outcomes include: total and cortical bone area (Tt.A and Ct.Ar, mm^2), cortical total volume (Ct.TV, mm^3), cortical bone volume (Ct.BV, mm^3), cortical bone mineral density (Ct.BMD, mg HA/cm^3), cortical tissue mineral density (Ct.TMD, mg HA/cm^3), apparent cortical thickness (Apparent Ct.Th, μm), fine cortical thickness (Fine Ct.Th, μm), cortical porosity (Ct.Po, %), pore volume (CtPo.V, mm^3), and pore diameter (Ct.Po.Dm, μm). Precision errors in our lab ranged from a root-mean squared coefficient of variation (CV%$_{RMS}$) of 1 to 8% for standard evaluation outcomes and from 1% to 11% for advanced cortical evaluation outcomes at the radius and tibia in 32 TDC with a mean age of 11.3y (Kawalilak et al., 2017).

For the purposes of my thesis, I will define bone size as total, cortical, and trabecular area and/or volume outcomes as: Tt.Ar, Ct.Ar, Ct.TV, Ct. BV, and Tb.Ar. I will define bone density as total, cortical, and trabecular bone and/or tissue mineral density outcomes as: Tt.BMD, Ct.BMD, Ct.TMD, and Tb.BMD. I will define cortical micro-architecture as: Apparent Ct.Th, Fine Ct.Th, Ct.Po, Ct.Po.V, and Ct.Po.Dm; and trabecular micro-architecture as: BV/TV, Tb.N, Tb.Th, Tb.Sp, and Tb.Sp.SD. These definitions are based on a recent study from our lab and I

will herein refer to all these outcomes together as bone size, density, and cortical and trabecular micro-architecture (Bunyamin et al., 2019).

4.4 Accelerometer Measurement

I measured daily minutes of MVPA, VPA, and impact counts ≥3.9g using a triaxial accelerometer (model wGT3X-BT, ActiGraph). Participants were instructed to wear the accelerometer on their right hip (mid-axillary line) attached using an elastic waist belt for 7 days. They were asked to only wear the belt while they were awake, and to remove the belt while they were sleeping, or during activities that may damage the accelerometer, such as water activities or contact sports. I analyzed accelerometer data based on a systematic review of recommendations for accelerometer data processing for children and adolescents (Migueles, Cadenas-Sanchez, Ekelund et al., 2017) using software provided by the manufacturer (ActiLife, v6.13.2). They recommended using a sampling frequency of 90-100Hz, however data previously collected from our sample of TDC was recorded at 30Hz (Kehrig et al., 2019), so I continued to record at 30Hz. Migueles et al. (2017) stated that they could not recommend a definition of non-wear time for children and adolescents. Based on visual inspection of wear time graphs output by ActiLife software, I chose to use the Choi et al. (2011) algorithm (Choi, Liu, Matthews et al., 2011), as those graphs adequately matched the wear time reported in each child's physical activity log. This algorithm defines non-wear time as consecutive zero counts for at least 90 minutes, allowing for short time intervals with non-zero counts up to 2 minutes (Choi et al., 2011). If no counts were recorded 30 minutes before and after the 2-minute time interval, this period of time is defined as non-wear (Choi et al., 2011). I was unable to match the wear-time criteria recommendation defining a valid week of accelerometer wear (≥4 days, ≥10 hours per day

(Migueles et al., 2017)). To allow for more participants in my sample, I used a less restrictive wear time criteria of at least 3 days with a minimum of 8 hours per day, including 1 day on the weekend (Sioen, Michels, Polfliet et al., 2015). I excluded accelerometer recordings that did not meet this wear time criteria. Activity counts were stored in 10 second intervals based on previous recommendations (Migueles et al., 2017). The thresholds for moderate PA (2296-4011 counts per minute, cpm) and VPA (≥4012 cpm) were originally validated using indirect calorimetry (estimated VO^2) exercise testing on a treadmill in children aged 5 to 8 years (Evenson et al., 2008), and have since been validated for use in older children and adolescents (Trost et al., 2011). This is important to note, as the thresholds identifying different intensities of physical activity are based on metabolic factors and have not been directly linked to mechanical loading of bone.

To measure daily impacts, I obtained the raw accelerometer data using the feature extraction tool from the manufacturer's software. I used Microsoft Excel Office 365 (version 1908) to count the total number of impact counts as the number of instances the peak resultant acceleration was equal to, or greater than a resultant acceleration of 3.9g on days with a valid wear time (Kehrig et al., 2019). The accelerometer was set to sample the peak acceleration value every 10 seconds (Kehrig et al., 2019). I calculated daily minutes of MVPA, VPA, and daily impact counts as the total minutes of MVPA and VPA, or total number of impact counts divided by the number of days of valid wear.

4.5 Forearm and Lower Leg Cross-Sectional Muscle Area

Another technician and I measured cross-sectional muscle area (mm^2) at shaft sites of the dominant forearm (65% ulna length) and lower leg (66% tibia length) using peripheral quantitative computed tomography (pQCT) (XCT 2000, Stratec Medizintechnik GmbH). Prior to imaging the radius and tibia shaft, another technician or I acquired a scout view of the distal radius or tibia and placed a reference line at the growth plate. If the scan quality was graded poorly (rating 4 or 5), mainly due to excessive patient movement, I excluded the scan from my analyses (Duff et al., 2017). We analyzed the image data using the manufacturer's software (version 6.00B). Cross-sectional muscle areas from the forearm and lower leg scans were obtained using contour mode 1 with a threshold of 40 mg/cm^3 to separate muscle from subcutaneous fat. Short-term precision of forearm and lower leg cross-sectional muscle area was previously calculated in 31 children. $CV\%_{RMS}$ values were reported as 2.8% and 3.6%, respectively (Björkman et al., 2017).

4.6 Statistical Methods

I reported the means and standard deviations of the background characteristics in the DM1 and TDC groups and assessed for significant differences in these characteristics between groups using independent *t*-tests. I identified outliers as values outside two standard deviations from the group mean using box plots and verified that these values were all correctly entered in the data sheet but did not remove them from my analyses.

4.6.1 Assumptions Testing

I tested the assumptions of normality, independence of observations, homogeneity of variance, and homogeneity of covariances prior to my analyses. I assessed normality of my variables using Q-Q plots and identified any outliers in my data using box plots. I found that daily minutes of VPA, daily impacts, Ct.Ar, Ct.TV, Ct.BV, Apparent Ct.Th, Fine Ct.Th, and Tb.Sp.SD at the radius, and Ct.TMD, Apparent Ct.Th, and Fine Ct.Th at the tibia were not normally distributed. The Durbin Watson statistic was approximately 2 in all of my models, indicating that there was an independence of observations. I tested for homogeneity of error variances using Levene's test. I found that apparent Ct.Th and Co.Po violated this assumption in the base model at the radius, but no variables violated this assumption in the base model at the tibia. Since several of my variables violated the assumption of normality or homogeneity of variances, I applied a natural logarithmic transformation to those variables and re-tested these assumptions. All transformed variables met the assumptions of normality and homogeneity of variances, so I re-ran analyses for my primary and secondary objectives including transformed variables in my models to address any potential errors caused by violating these assumptions (Appendix). However, due to challenges in the interpretation of logarithmic data, I chose to report my findings without log transformations in my results and have provided findings from my models including transformed variables in the appendix due to challenges in the interpretation of logarithmic data. Findings were comparable between transformed and non-transformed data. (Appendix, Figure 7).

4.6.2 Using Sex, Maturity, Site-Specific Muscle Area, and BMI z-score as Covariates

I chose to adjust for sex, years from aPHV (maturity), site-specific muscle area, and BMI z-score (body size) in my models since these variables are reported determinants of bone characteristics in children (Gabel et al., 2017a; Kehrig et al., 2019). Since there was a significant difference in

chronological age and maturity between DM1 and TDC groups, I chose to adjust for years from aPHV, to account for variation in the somatic maturity, particularly long bone growth, between participants (Bunyamin et al., 2019).

There was no difference in the distribution of boys and girls between DM1 and TDC groups, assessed using Chi-square, however all covariates (including sex) were significant factors influencing the variance in bone micro-architecture in my models.

4.6.3 Multivariate Analysis and Pairwise Comparisons of Bone Size, Density, and Micro-architecture Between Groups (Primary Objective)

For my primary objective, I used two site-specific MANCOVAs to compare bone size, density, and cortical and trabecular micro-architecture at the radius and tibia between children with DM1 and TDC after adjusting for sex, maturity (years from aPHV), site-specific muscle area, and BMI z-score. I reported the F-ratios (Pillai's trace) assessing differences between the groups in the radius and tibia models. For post hoc testing, I used pairwise comparisons with Bonferroni correction for multiple comparisons. I reported unadjusted group means and standard deviations, mean and percent differences in adjusted group means, and 95% confidence intervals of adjusted mean differences in bone size, density, and trabecular and cortical micro-architecture between children and youth with DM1 and TDC. Significance was set at $p<0.05$.

4.6.4 Assessing the Role of Daily MVPA, VPA, and Impacts (Secondary Objective)

For my secondary objective, I first used site-specific MANCOVAs to assess if daily minutes of MVPA, VPA, and daily impacts were factors influencing differences in bone size, density, and cortical and trabecular micro-architecture between the groups (children with DM1 vs. TDC). I used the radius and tibia MANCOVAs from my primary objective analyses as base models to address my secondary objective and included each PA variable as a fifth covariate in my radius

and tibia models. The role of PA was explored in two ways. First, I reported the standardized β-coefficients of the PA outcomes to assess the independent role of PA in the models of those bone outcomes that differed between DM1 and TDC groups; as assessed in my primary objective. I also reported standardized β-coefficients of the covariates; sex, maturity (years from aPHV), site-specific muscle area (forearm or lower leg), and BMI z-score. I chose to report standardized β-coefficients instead of unstandardized β-coefficients, as standardized β-coefficients are in units of standard deviations and allow for a direct comparison of the independent role of PA between bone outcomes. Reporting the standardized β-coefficients of my covariates also highlights the challenges associated with identifying which covariates should be included in multivariate models. I used an explanatory modeling approach (Shmueli, 2010) by reporting the standardized β-coefficients (the slope of the regression line) to predict the estimated change in standard deviations of the bone outcome per 1 standard deviation change in PA. Second, I reported results from pairwise comparisons (Bonferroni) to explore the role of PA on bone outcomes by illustrating group differences in bone outcomes between children and youth with DM1 and TDC before and after controlling for PA variables that significantly contributed to the model. I reported unadjusted group means and standard deviations, mean and percent differences in adjusted group means, and 95% confidence intervals of adjusted mean differences in bone size, density, and cortical and trabecular micro-architecture between children and youth with DM1 and TDC. Significance was set at $p<0.05$.

5 RESULTS

5.1 Background Characteristics

Descriptive background characteristics of participants are provided in Table 1. Independent *t*-tests showed that our sample of children and youth with DM1 were older (p=0.029) and more mature (p=0.035) than our sample of TDC (Table 2).

Table 2. Background characteristics of children and youth with DM1 and TDC.

	DM1			TDC			
	n	Mean	SD	n	Mean	SD	*p*-value
Number of girls (%)	21	12(57%)		47	22(47%)		
Age (years)	21	12.1	2.1	47	10.9	1.6	**0.029**
Age at PHV (years)	21	12.5	0.8	47	12.4	0.7	0.664
Years from age at PHV (years)	21	-0.4	2.1	47	-1.5	1.5	**0.035**
Height (cm)	21	152.2	12.4	47	147.9	12.5	0.200
Body mass (kg)	21	48.4	16.0	47	42.3	16.2	0.154
Body mass index	21	20.3	3.8	47	18.8	4.7	0.177
Body mass index z-score	21	0.53	0.92	47	0.16	1.2	0.158
Body mass index percentile (%)	21	68.2	26.8	47	54.2	30.7	0.063
Seated height (cm)	21	80.3	7.3	47	78.0	6.2	0.222
Leg length (cm)	21	71.9	5.5	47	69.9	6.9	0.213
Ulna length (mm)	21	240.3	21.9	47	236.3	22.9	0.495
Tibia length (mm)	21	349.3	28.5	47	356.4	35.6	0.384
Forearm muscle area (mm²)	21	2538.5	696.8	45	2272.4	663.5	0.151
Lower leg muscle area (mm²)	21	4668.8	1316.0	45	4409.5	1425.4	0.472
Daily protein intake (g/day)	21	75.3	40.2	34	61.2	30.8	0.175
Daily calcium intake (mg/day)	21	923.7	385.9	34	900.3	504.0	0.847
Daily vitamin D intake (IU/day)	21	139.9	105.7	34	191.4	163.2	0.161
Daily MVPA (min/day)	21	48.5	21.9	47	51.1	22.3	0.661
Daily VPA (min/day)	21	15.8	11.0	47	19.2	10.5	0.245
Daily impacts (# impacts/day)	21	47	52	47	73	59	0.073
Age at DM1 diagnosis (years)	21	6.8	2.2				
Years since DM1 diagnosis (years)	21	5.3	2.5				
HbA1c (%)	20	8.5	1.0				

5.2 Differences in Bone Size, Density, and Micro-Architecture Between Children with DM1 and TDC (Primary Objective)

There was a significant difference in bone size, density, and cortical and trabecular micro-architecture at the radius ($F(18,42)=7.594$, $p<0.001$) and a significant difference in cortical

micro-architecture at the tibia (F(18,42)=2.826, p=0.003) between children and youth with DM1 and TDC.

5.2.1 Pairwise Comparisons of Percent Differences in Bone Size, Density, and Micro-Architecture Between Groups

At the radius, children with DM1 had a lower total bone area (-13.3%), greater total BMD (+12.3%), cortical BMD (+9.3%), cortical TMD (+4.7%), apparent cortical thickness (+21.7%), fine cortical thickness (+22.7%); lower cortical porosity (-39.2%), pore volume (-33.6%), pore diameter (-11.1%), trabecular area (-18.2%), trabecular number (-6.1%); and greater trabecular separation (+7.0%) (Table 3, Figure 4).

At the tibia, children with DM1 had a lower cortical porosity (-22.5%), pore volume (-28.4%), and pore diameter (-6.7%) (Table 4, Figure 5).

Table 3. Descriptive statistics and adjusted[†] group differences in bone size, density, and micro-architecture at the radius between children and youth with type 1 diabetes (DM1) and typically developing children and youth (TDC).

	DM1 (n=20)		TDC (n=45)					
	Mean	SD	Mean	SD	*Adj Mean Diff	*95% CI of Adj Diff		*p-value
						Lower	Upper	
Tt.Ar (mm²)	193.3	43.3	208.4	41.0	**-28.3**	**-44.4**	**-12.1**	**0.001**
Tt.BMD (mg HA/cm³)	277.9	46.1	246.8	40.7	**30.4**	**8.7**	**52.0**	**0.007**
Ct.Ar (mm²)	41.5	12.8	39.7	7.4	-0.4	-4.2	3.5	0.846
Ct.TV (mm³)	374.7	115.1	358.2	66.3	-3.4	-38.1	31.4	0.846
Ct.BV (mm³)	336.1	114.3	282.1	54.0	31.8	-0.3	63.9	0.052
Ct.BMD (mg HA/cm³)	771.0	62.8	690.5	52.4	**65.0**	**37.4**	**92.6**	**<0.001**
Ct.TMD (mg HA/cm³)	811.8	55.1	762.6	35.3	**35.7**	**15.0**	**56.3**	**0.001**
Apparent Ct.Th (µm)	755.9	208.5	593.0	105.7	**131**	**58.4**	**202.9**	**0.001**
Fine Ct.Th (µm)	496.6	120.9	384.6	51.4	**89**	**47.7**	**129.9**	**<0.001**
Ct.Po (%)	4.2	1.8	7.6	2.8	**-2.9**	**-4.1**	**-1.6**	**<0.001**
Ct.Po.V (mm³)	14.3	8.4	23.0	11.8	**-7.6**	**-12.6**	**-2.6**	**0.004**
Ct.Po.Dm (µm)	143	7.1	162	9.9	**-18**	**-21.8**	**-12.9**	**<0.001**
Tb.Ar (mm²)	154.8	37.5	177.4	38.8	**-32.9**	**-49.9**	**-15.9**	**<0.001**
Tb.BMD (mg HA/cm³)	166.0	28.8	179.1	34.4	-7.8	-23.5	7.9	0.323
BV/TV (%)	13.8	2.4	14.9	2.9	-0.7	-2.0	0.7	0.322
Tb.N (1/mm)	2.1	0.2	2.3	0.2	**-0.1**	**-0.3**	**0.0**	**0.028**
Tb.Th (µm)	66	8.7	66	9.7	1	-3.5	6.0	0.606
Tb.Sp (µm)	416	51.4	381	51.0	**27**	**0.7**	**53.7**	**0.044**

Tb.Sp.SD (μm)	163	26.5	147	32.3	10	-6.4	25.5	0.237

Abbreviations: Tt.Ar = total bone area, Tt.BMD = total bone mineral density, Ct.Ar = cortical area, Ct.TV = cortical total volume, Ct.BV = cortical bone volume, Ct.BMD = cortical bone mineral density, Ct.TMD = cortical tissue mineral density, Ct.Th = cortical thickness, Ct.Po = cortical porosity, Ct.Po.V = cortical pore volume, Ct.Po.Dm = cortical pore diameter, Tb.Ar = trabecular area, Tb.BMD = trabecular bone mineral density, BV/TV = trabecular bone volume fraction, Tb.N = trabecular number, Tb.Th = trabecular thickness, Tb.Sp = trabecular separation, Tb.Sp.SD = trabecular heterogeneity. *Bonferroni adjustment for multiple comparisons. †Covariates were evaluated as sex (girls=1, boys=2), years from age at PHV = -1.17y, forearm muscle area = 2327.4 mm², and BMI z-score = 0.27.

Figure 4. Percent differences in bone size, density, and micro-architecture at the radius between children and youth with type 1 diabetes (DM1) and typically developing children and youth (TDC) after adjusting for sex, years from estimated age at peak height velocity, forearm muscle area, and BMI z-score.

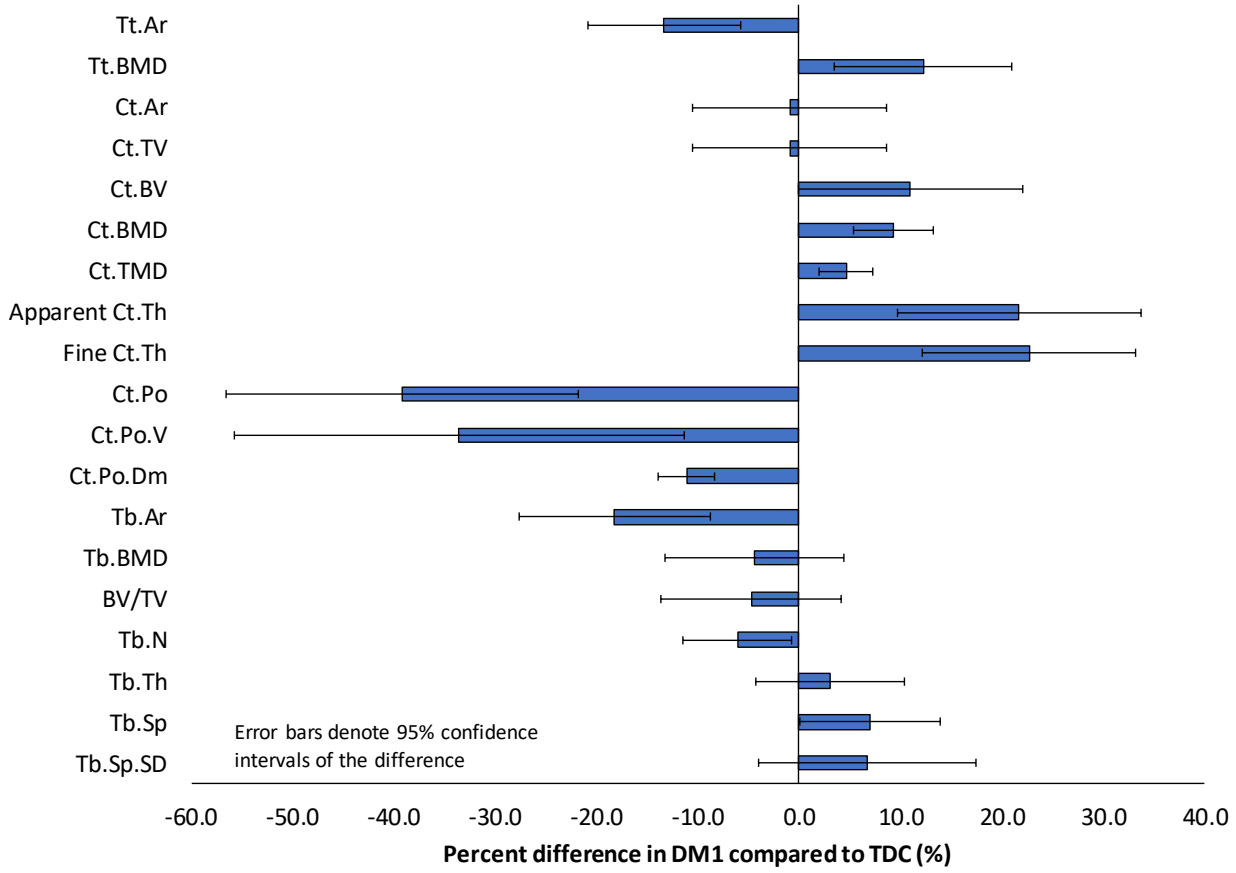

Abbreviations: Tt.Ar = total bone area, Tt.BMD = total bone mineral density, Ct.Ar = cortical area, Ct.TV = cortical total volume, Ct.BV = cortical bone volume, Ct.BMD = cortical bone mineral density, Ct.TMD = cortical tissue mineral density, Ct.Th = cortical thickness, Ct.Po = cortical porosity, Ct.Po.V = cortical pore volume, Ct.Po.Dm = cortical pore diameter, Tb.Ar = trabecular area, Tb.BMD = trabecular bone mineral density, BV/TV = trabecular bone volume fraction, Tb.N = trabecular number, Tb.Th = trabecular thickness, Tb.Sp = trabecular separation, Tb.Sp.SD = trabecular heterogeneity.

Table 4. Descriptive statistics and adjusted† group differences in bone size, density, and micro-architecture at the tibia between children and youth with type 1 diabetes (DM1) and typically developing children and youth (TDC).

	DM1 (n=20)		TDC (n=45)					
	Mean	SD	Mean	SD	*Adj Mean Diff	*95% CI of Adj Diff		*p-value
						Lower	Upper	
Tt.Ar (mm²)	682.3	107.0	673.4	115.3	-40.6	-89.8	8.7	0.104
Tt.BMD (mg HA/cm³)	239.3	32.5	236.4	31.6	-0.8	-18.4	16.9	0.930
Ct.Ar (mm²)	80.3	20.2	78.9	16.5	-7.1	-15.2	1.1	0.088
Ct.TV (mm³)	723.9	182.3	711.9	149.2	-63.8	-137.5	9.8	0.088
Ct.BV (mm³)	629.9	176.7	585.8	128.7	-30.2	-96.1	35.8	0.364
Ct.BMD (mg HA/cm³)	757.3	73.6	719.1	42.0	14.4	-15.1	43.9	0.333
Ct.TMD (mg HA/cm³)	813.5	64.2	788.8	33.1	0.7	-22.3	23.7	0.953
Apparent Ct.Th (µm)	751.0	184.5	683.1	0.2	-3	-91.0	85.9	0.954
Fine Ct.Th (µm)	435.8	93.1	389.5	0.0	20	-16.4	56.5	0.276
Ct.Po (%)	6.1	2.3	8.0	0.0	**-1.8**	**-3.2**	**-0.3**	**0.018**
Ct.Po.V (mm³)	40.4	17.8	52.0	23.8	**-15.1**	**-27.6**	**-2.6**	**0.018**
Ct.Po.Dm (µm)	152	7.9	163	0.0	**-11**	**-15.8**	**-5.4**	**<0.001**
Tb.Ar (mm²)	607.9	96.4	601.5	111.3	-41.1	-90.5	8.2	0.101
Tb.BMD (mg HA/cm³)	180.4	19.0	187.5	24.4	-5.3	-18.4	7.8	0.422
BV/TV (%)	15.0	1.6	15.6	0.0	-0.5	-1.5	0.6	0.414
Tb.N (1/mm)	2.1	0.2	2.1	0.3	0.0	-0.1	0.1	0.964
Tb.Th (µm)	74	9.5	76	0.0	-3	-9.0	3.3	0.353
Tb.Sp (µm)	416	42.7	412	0.1	-2	-33.1	29.2	0.901
Tb.Sp.SD (µm)	174	30.8	170	0.0	-2	-21.5	17.2	0.822

Abbreviations: Tt.Ar = total bone area, Tt.BMD = total bone mineral density, Ct.Ar = cortical area, Ct.TV = cortical total volume, Ct.BV = cortical bone volume, Ct.BMD = cortical bone mineral density, Ct.TMD = cortical tissue mineral density, Ct.Th = cortical thickness, Ct.Po = cortical porosity, Ct.Po.V = cortical pore volume, Ct.Po.Dm = cortical pore diameter, Tb.Ar = trabecular area, Tb.BMD = trabecular bone mineral density, BV/TV = trabecular bone volume fraction, Tb.N = trabecular number, Tb.Th = trabecular thickness, Tb.Sp = trabecular separation, Tb.Sp.SD = trabecular heterogeneity. *Bonferroni adjustment for multiple comparisons. †Covariates were evaluated as sex (girls=1, boys=2), years from age at PHV = -1.1y, lower leg muscle area = 4519.9 mm², and BMI z-score = 0.27.

Figure 5. Percent differences in bone size, density, and micro-architecture at the tibia between children and youth with type 1 diabetes (DM1) and typically developing children and youth (TDC) after adjusting for sex, years from estimated age at peak height velocity, lower leg muscle area, and BMI z-score.

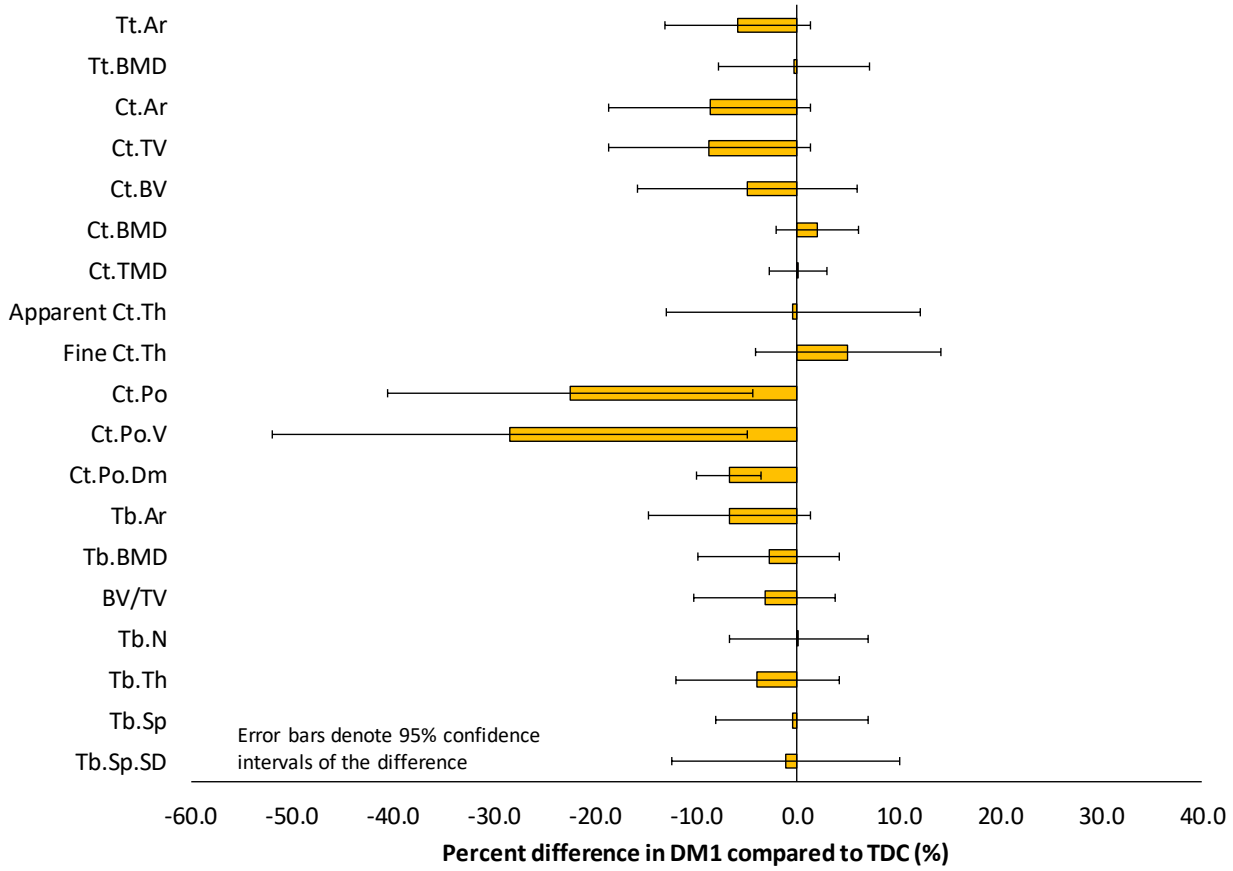

Abbreviations: Tt.Ar = total bone area, Tt.BMD = total bone mineral density, Ct.Ar = cortical area, Ct.TV = cortical total volume, Ct.BV = cortical bone volume, Ct.BMD = cortical bone mineral density, Ct.TMD = cortical tissue mineral density, Ct.Th = cortical thickness, Ct.Po = cortical porosity, Ct.Po.V = cortical pore volume, Ct.Po.Dm = cortical pore diameter, Tb.Ar = trabecular area, Tb.BMD = trabecular bone mineral density, BV/TV = trabecular bone volume fraction, Tb.N = trabecular number, Tb.Th = trabecular thickness, Tb.Sp = trabecular separation, Tb.Sp.SD = trabecular heterogeneity.

5.3 Role of Daily MVPA, VPA, and Impacts on Bone Size, Density and Micro-Architecture in Children with DM1 and TDC (Secondary Objective)

Daily minutes of VPA independently predicted the variance in cortical pore diameter at the radius (Std. β=-0.18, *p*=0.033), but did not independently predict the variance in total bone area,

total or cortical BMD, cortical TMD, apparent or fine cortical thickness, cortical porosity, pore volume, trabecular area, number, or separation (Table 5). Daily minutes of MVPA and daily impacts did not contribute to the overall variance in bone size, density, and micro-architecture at the radius (p=0.650, p=0.131) or at the tibia (p=0.417, p=0.791), respectively.

Table 5. Standardized β-coefficients of base model covariates and daily minutes of vigorous physical activity (VPA) for bone size, density, and micro-architecture at the radius in a pooled sample of children and youth with type 1 diabetes (DM1) and typically developing children and youth (TDC).

		Std. β	*p*-value
Tt.Ar	Sex	0.26	0.040
	Maturity (years from aPHV)	0.59	<0.001
	Forearm muscle area	0.29	0.073
	Body mass index z-score	0.01	0.952
	Daily VPA	0.16	0.076
	Group (DM1 and TDC)	-0.30	0.001
Tt.BMD	Sex	-0.01	0.932
	Maturity (years from aPHV)	-0.26	0.189
	Forearm muscle area	0.56	0.010
	Body mass index z-score	-0.02	0.881
	Daily VPA	-0.06	0.583
	Group (DM1 and TDC)	0.31	0.009
Ct.BMD	Sex	0.18	0.180
	Maturity (years from aPHV)	0.44	0.010
	Forearm muscle area	-0.37	0.042
	Body mass index z-score	0.51	<0.001
	Daily VPA	-0.04	0.698
	Group (DM1 and TDC)	0.45	<0.001
Ct.TMD	Sex	0.17	0.242
	Maturity (years from aPHV)	0.48	0.007
	Forearm muscle area	-0.20	0.274
	Body mass index z-score	0.40	0.004
	Daily VPA	-0.13	0.199
	Group (DM1 and TDC)	0.33	0.002
Apparent Ct.Th	Sex	0.14	0.327
	Maturity (years from aPHV)	0.28	0.119
	Forearm muscle area	0.21	0.266
	Body mass index z-score	0.05	0.694
	Daily VPA	-0.18	0.083
	Group (DM1 and TDC)	0.36	0.001
Fine Ct.Th	Sex	0.15	0.290
	Maturity (years from aPHV)	0.50	0.006
	Forearm muscle area	-0.28	0.139
	Body mass index z-score	0.28	0.036
	Daily VPA	-0.17	0.094
	Group (DM1 and TDC)	0.42	<0.001
Ct.Po	Sex	-0.10	0.465

	Maturity (years from aPHV)	-0.44	0.015
	Forearm muscle area	0.69	<0.001
	Body mass index z-score	-0.54	<0.001
	Daily VPA	-0.04	0.730
	Group (DM1 and TDC)	-0.45	<0.001
Ct.Po.V	Sex	-0.07	0.603
	Maturity (years from aPHV)	-0.46	0.012
	Forearm muscle area	0.95	<0.001
	Body mass index z-score	-0.49	0.001
	Daily VPA	-0.06	0.551
	Group (DM1 and TDC)	-0.31	0.003
Ct.Po.Dm	Sex	-0.03	0.808
	Maturity (years from aPHV)	-0.12	0.377
	Forearm muscle area	0.37	0.014
	Body mass index z-score	-0.55	<0.001
	Daily VPA	**-0.18**	**0.033**
	Group (DM1 and TDC)	-0.66	<0.001
Tb.Ar	Sex	0.21	0.122
	Maturity (years from aPHV)	0.51	0.004
	Forearm muscle area	0.26	0.149
	Body mass index z-score	-0.03	0.794
	Daily VPA	0.19	0.060
	Group (DM1 and TDC)	-0.37	<0.001
Tb.N	Sex	-0.36	0.034
	Maturity (years from aPHV)	-0.68	0.002
	Forearm muscle area	0.65	0.004
	Body mass index z-score	-0.12	0.437
	Daily VPA	0.05	0.653
	Group (DM1 and TDC)	-0.26	0.033
Tb.Sp	Sex	0.33	0.049
	Maturity (years from aPHV)	0.71	0.001
	Forearm muscle area	-0.71	0.002
	Body mass index z-score	0.16	0.307
	Daily VPA	-0.08	0.492
	Group (DM1 and TDC)	0.23	0.054

Abbreviations: Tt.Ar = total bone area, Tt.BMD = total bone mineral density, Ct.Ar = cortical area, Ct.TV = cortical total volume, Ct.BV = cortical bone volume, Ct.BMD = cortical bone mineral density, Ct.TMD = cortical tissue mineral density, Ct.Th = cortical thickness, Ct.Po = cortical porosity, Ct.Po.V = cortical pore volume, Ct.Po.Dm = cortical pore diameter, Tb.Ar = trabecular area, Tb.BMD = trabecular bone mineral density, BV/TV = trabecular bone volume fraction, Tb.N = trabecular number, Tb.Th = trabecular thickness, Tb.Sp = trabecular separation, Tb.Sp.SD = trabecular heterogeneity.

Pairwise comparisons revealed that group differences in radius bone size, density, cortical and trabecular micro-architecture between children with DM1 and TDC remained after adjusting for daily minutes of VPA, excluding trabecular separation (p=0.054) (Table 6). After adjusting for VPA, children with DM1 had a lower total bone area (-12.6%); greater total BMD (+12.0%), cortical BMD (+9.3%), cortical TMD (+4.5%), apparent cortical thickness (+20.5%),

fine cortical thickness (+21.6%); and a lower cortical porosity (-39.2%), pore volume (-34.2%), pore diameter (-11.1%), trabecular area (-17.4%), and number (-6.0%) at the radius (Table 6, Figure 6).

Table 6. Descriptive statistics of bone size, density, and micro-architecture at the radius between children and youth with type 1 diabetes (DM1) and typically developing children and youth (TDC). Adjusting[†] for covariates in base model, as well as daily minutes of vigorous physical activity (VPA).

	DM1 (n=20)		TDC (n=45)					
	Mean	SD	Mean	SD	*Adj Mean Diff	*95% CI of Adj Diff		*p-value
						Lower	Upper	
Tt.Ar (mm²)	193.3	43.3	208.4	41.0	**-26.8**	**-42.7**	**-10.9**	**0.001**
Tt.BMD (mg HA/cm³)	277.9	46.1	246.8	40.7	**29.8**	**7.9**	**51.6**	**0.009**
Ct.Ar (mm²)	41.5	12.8	39.7	7.4	-0.6	-4.5	3.2	0.739
Ct.TV (mm³)	374.7	115.1	358.2	66.3	-5.8	-40.5	28.9	0.739
Ct.BV (mm³)	336.1	114.3	282.1	54.0	29.6	-2.5	61.6	0.070
Ct.BMD (mg HA/cm³)	771.0	62.8	690.5	52.4	**64.4**	**36.5**	**92.4**	**<0.001**
Ct.TMD (mg HA/cm³)	811.8	55.1	762.6	35.3	**34.3**	**13.7**	**54.9**	**0.002**
Apparent Ct.Th (µm)	755.9	208.5	593.0	105.7	**124**	**0.1**	**0.2**	**0.001**
Fine Ct.Th (µm)	496.6	120.9	384.6	51.4	**85**	**0.0**	**0.1**	**<0.001**
Ct.Po (%)	4.2	1.8	7.6	2.8	**-2.9**	**0.0**	**0.0**	**<0.001**
Ct.Po.V (mm³)	14.3	8.4	23.0	11.8	**-7.8**	**-12.8**	**-2.7**	**0.003**
Ct.Po.Dm (µm)	143	7.1	162	9.9	**-18**	**0.0**	**0.0**	**<0.001**
Tb.Ar (mm²)	154.8	37.5	177.4	38.8	**-31.3**	**-48.0**	**-14.5**	**<0.001**
Tb.BMD (mg HA/cm³)	166.0	28.8	179.1	34.4	-7.3	-23.2	8.6	0.360
BV/TV (%)	13.8	2.4	14.9	2.9	-0.6	0.0	0.0	0.359
Tb.N (1/mm)	2.1	0.2	2.3	0.2	**-0.1**	**-0.3**	**0.0**	**0.033**
Tb.Th (µm)	66	8.7	66	9.7	1	0.0	0.0	0.573
Tb.Sp (µm)	416	51.4	381	51.0	26	0.0	0.1	0.054
Tb.Sp.SD (µm)	163	26.5	147	32.3	9	0.0	0.0	0.260

Abbreviations: Tt.Ar = total bone area, Tt.BMD = total bone mineral density, Ct.Ar = cortical area, Ct.TV = cortical total volume, Ct.BV = cortical bone volume, Ct.BMD = cortical bone mineral density, Ct.TMD = cortical tissue mineral density, Ct.Th = cortical thickness, Ct.Po = cortical porosity, Ct.Po.V = cortical pore volume, Ct.Po.Dm = cortical pore diameter, Tb.Ar = trabecular area, Tb.BMD = trabecular bone mineral density, BV/TV = trabecular bone volume fraction, Tb.N = trabecular number, Tb.Th = trabecular thickness, Tb.Sp = trabecular separation, Tb.Sp.SD = trabecular heterogeneity. *Bonferroni adjustment for multiple comparisons. [†]Covariates were evaluated as sex (girls=1, boys=2), years from age at PHV = -1.17, forearm muscle area = 2327.4 mm², BMI z-score = 0.27, and VPA = 18.5 minutes/day.

Figure 6. Percent differences in bone size, density, and micro-architecture at the radius between children and youth with type 1 diabetes (DM1) and typically developing children and youth (TDC) in the base model without adjusting for vigorous physical activity (VPA) and after adjusting for VPA.

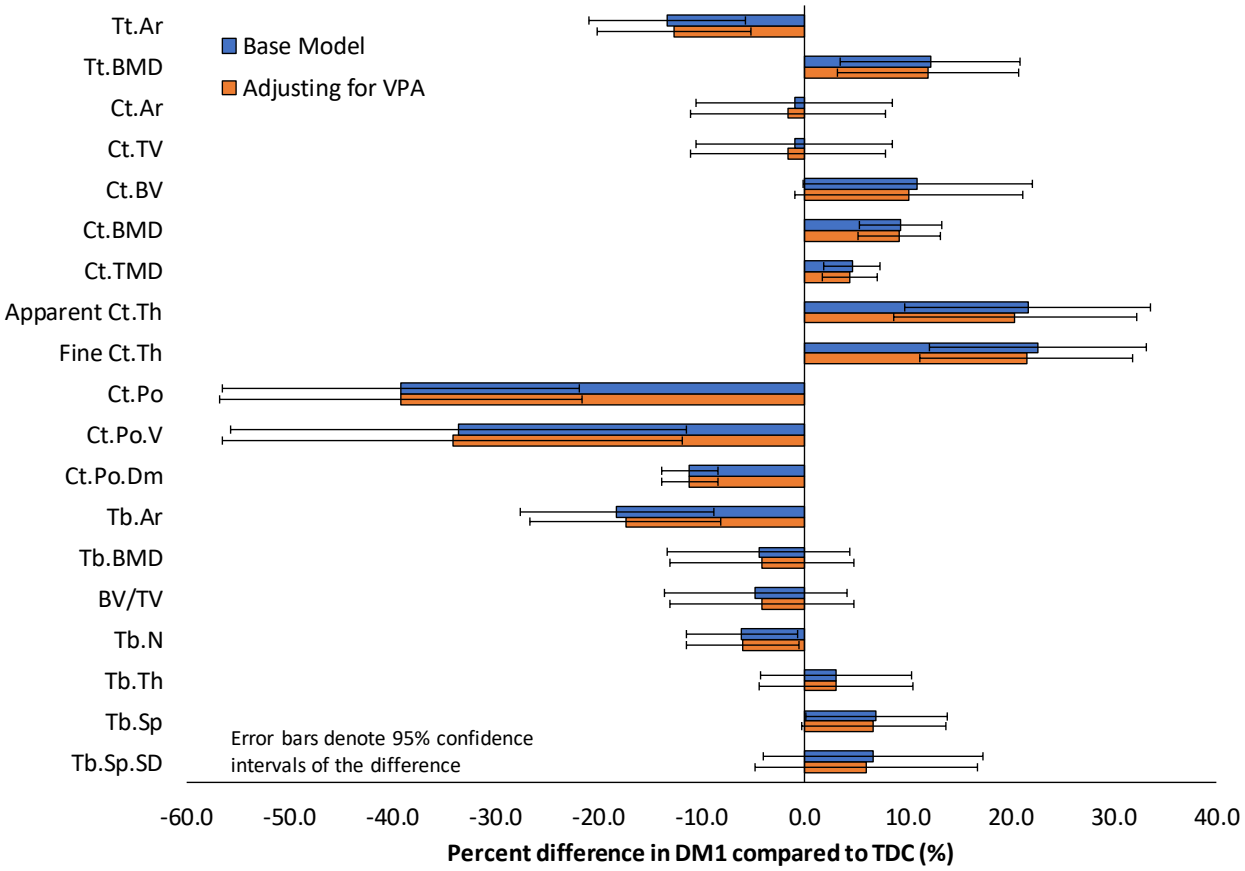

Abbreviations: Tt.Ar = total bone area, Tt.BMD = total bone mineral density, Ct.Ar = cortical area, Ct.TV = cortical total volume, Ct.BV = cortical bone volume, Ct.BMD = cortical bone mineral density, Ct.TMD = cortical tissue mineral density, Ct.Th = cortical thickness, Ct.Po = cortical porosity, Ct.Po.V = cortical pore volume, Ct.Po.Dm = cortical pore diameter, Tb.Ar = trabecular area, Tb.BMD = trabecular bone mineral density, BV/TV = trabecular bone volume fraction, Tb.N = trabecular number, Tb.Th = trabecular thickness, Tb.Sp = trabecular separation, Tb.Sp.SD = trabecular heterogeneity.

6 DISCUSSION

6.1 Differences in Bone Size, Density, and Micro-Architecture Between Children with DM1 and TDC

6.1.1 Total and Cortical Bone Size and Density, and Cortical Micro-Architecture

The results of my primary objective suggest that children with DM1 had 11-39% lower total area, cortical porosity, pore volume, and pore diameter, and 5-23% greater total BMD, cortical BMD, cortical TMD, and apparent and fine cortical thicknesses compared to the TDC group at the radius, and 7-28% lower cortical porosity, pore volume, and pore diameter at the tibia after adjusting for sex, maturity, site-specific muscle area (forearm or lower leg), and BMI z-score. Observed smaller bone size (Bechtold et al., 2007; Roggen et al., 2013; Saha et al., 2009), and greater cortical densities (Maratova et al., 2018) in children with DM1 agree with most of the previous literature whereas my observations of a thicker and less porous cortical micro-architecture were not reported in previous literature (Table 1). At its surface, these findings do not appear to fit into the narrative of higher fracture rates in children with DM1. Based on mechanical test data, a denser and thicker cortical bone structure is thought to be more structurally favourable (Muller et al., 2008). This study found that cortical thickness was a better predictor of bone failure load than total BMD at the radius shaft, where cortical thickness predicted 72% of the variance in failure load compared to 42% of the variance predicted by total BMD (Muller et al., 2008).

However, it is still possible that children with DM1 may present with a structurally beneficial cortical bone micro-architecture may still be subject to a greater fracture risk than TDC, as total and trabecular bone size, density, and trabecular micro-architecture may play a more important role for resisting fractures at distal regions of long bones (Chevalley, Bonjour,

van Rietbergen et al., 2011; Kontulainen, Johnston, Liu et al., 2008). Previous mechanical test data found that compressive bone strength, estimated as a product of total bone area and total density squared, predicted up to 85% of the variance in compressive failure load at the distal tibia (Kontulainen et al., 2008). Findings from a prospective study of 176 boys found that boys with fractures had a lower trabecular BMD and trabecular number, but not cortical BMD or thickness, compared to boys without fractures (Chevalley et al., 2011). It is important to make the distinction that I am reporting cortical bone characteristics at the distal region of the radius and tibia, whereas cortical bone findings derived from pQCT studies measured cortical bone properties at shaft sites of the radius or tibia.

From a cross-sectional point of view, several studies reported a lower cortical area, content and/or thickness (Maratova et al., 2018; Moyer-Mileur et al., 2004; Saha et al., 2009), or density (Bechtold et al., 2007; Weber, Gordon, Kelley et al., 2019) in children with DM1. These findings seem contradictory to those presented in my thesis. However, other studies either reported no significant differences in cortical density (Heap et al., 2004; Lettgen et al., 1995; Saha et al., 2009), and cortical area (Heap et al., 2004), or reported a greater cortical density in children with DM1, similar to my own findings (Maratova et al., 2018; Moyer-Mileur et al., 2004). Interestingly, Moyer-Mileur et al. (2004) reported lower gains in cortical bone area, content, density, and torsional bone strength (compared to predicted change data of TDC) in children with DM1 despite reporting a greater cortical density at baseline (Moyer-Mileur et al., 2004). Findings from Moyer-Mileur et al. (2004) may be explained by previous evidence from an experimental study in osteoblasts. This study found that higher glucose concentrations speed up the mineralization process of bone, along with a reduced bone mineral quality (Garcia-

Hernandez, Arzate, Gil-Chavarria et al., 2012). This may help to explain why children with DM1 in my study had a greater total and cortical BMD, cortical TMD, and cortical thicknesses.

As there is limited evidence observing differences in total and cortical bone properties between children and youth with DM1 and TDC, discrepancies of my thesis findings compared to previous literature may be explained by differences in ages between participants, the use of pQCT instead of HR-pQCT, and measuring cortical outcomes at the tibia shaft, instead of at the radius. First, three of the studies that reported lower cortical densities or thicknesses studied adolescents with a mean age of 14-16y (Maratova et al., 2018; Moyer-Mileur et al., 2004; Weber et al., 2019), compared to the younger mean age my participants (11.3y). Three studies that disagreed with my findings and reported lower densities or cortical thicknesses measured these outcomes at the tibia shaft using pQCT (Maratova et al., 2018; Moyer-Mileur et al., 2004; Weber et al., 2019), instead of at the distal radius using HR-pQCT. It is more common to only measure cortical bone properties at shaft sites using pQCT, instead of at the distal region using HR-pQCT. As bone adaptation is site-specific, there are also site-specific variations in bone properties at the weight-bearing tibia compared to the non-weight-bearing radius in children (D. Liu et al., 2010). Due to a limited number of studies assessing bone in children and youth with DM1, I am not able to directly compare my thesis findings to previous studies without running into issues of external validity.

6.1.2 Trabecular Bone Size, Density, and Trabecular Micro-Architecture

The results of my primary objective suggest that children with DM1 had 18% lower trabecular area, 6% lower trabecular number, and 7% greater trabecular separation compared to the TDC group at the radius, but no differences at the tibia after adjusting for sex, maturity, site-specific muscle area (forearm or lower leg), and BMI z-score. These trabecular bone findings agree with

the previous study reporting an 8% lower trabecular number and 13% greater trabecular separation, as well as a 7% lower trabecular bone volume fraction in children with DM1 using MRI at the proximal end of the tibia (Chen et al., 2019).

Other studies did not assess trabecular bone micro-architecture, but their findings follow a similar pattern of DM1-related deficits in trabecular bone size and/or density (Heap et al., 2004; Lettgen et al., 1995; Maratova et al., 2018; Moyer-Mileur et al., 2004; Saha et al., 2009; Weber et al., 2019). In contrast to these previous studies, Bechtold et al. (2007) reported a higher trabecular density in children with DM1 (mean age=9.9y). However, a major limitation of this study was that these differences were compared to normative data, z-scores, and predicted changes of a typically-developing reference population. They interpreted their findings based on normative data, and also stated that DM1-related differences in bone characteristics had normalized after 5.5 years (Bechtold et al., 2007). Differences in my thesis findings may be due to the younger age at which baseline measurements were recorded (9.9y mean age) in this study. Most of the children in Bechtold et al. (2007) were pre-pubertal (27 of 41 total), and these children had a lower mean length of DM1 diagnosis was (4.3y at baseline) compared to my sample (5.3y). Site-specific differences in weight-bearing (tibia) and non-weight-bearing (radius) sites (D. Liu et al., 2010) may also explain why DM1-related deficits in total bone size, density, trabecular area, and trabecular micro-architecture were only present at the radius. I suggest that the weight-bearing activity at the tibia may have provided enough of a mechanical loading stimulus, to be protective against DM1-related metabolic differences, mostly as a result of hyperglycaemia, and potentially underlying the deficits observed at the non-weight-bearing radius. Overall, observed deficits in trabecular number and a greater trabecular separation

suggest a weaker trabecular bone morphology at the radius in children with DM1, which may underpin higher fracture rates, particularly at the wrist.

6.2 Role of PA on Bone Size, Density, and Micro-Architecture

The results of my secondary objective show that daily minutes of VPA independently predicted cortical pore diameter at the radius (Std. β=-0.18, p=0.033). This finding suggests a negative relationship between daily VPA and cortical pore diameter, however due to the low sample size of children with DM1 (n=21), I did not have power to test if there was an interaction between group and PA. I assessed a mixed-cohort of children with DM1 and TDC, so it is still unclear if this relationship is different between groups. Pairwise comparisons revealed that after controlling for daily minutes of VPA, there were still significant differences in bone outcomes between DM1 and TDC groups. However, trabecular separation was no longer significantly different between groups and there was only a very slight change in the magnitude of percent differences between groups (ranged from -0.7% to 1.2%) after adjusting for daily VPA. Trabecular separation not remaining as significantly different between groups after controlling for VPA is likely a result of a loss in statistical power after controlling for an additional covariate. This increased my likelihood of a type II error as the p-value for trabecular separation changed from p=0.044 to 0.054 (Table 3, Table 6). Further, after applying logarithmic transformations to variables that were not normally distributed; including daily minutes of VPA, daily minutes of VPA also independently predicted the variance in cortical TMD and fine cortical thickness (Appendix, Table 9 pg. 63-65).

Previous PA studies report a beneficial relationship between MVPA, VPA and/or impacts and bone outcomes at the weight-bearing tibia (Gabel et al., 2017b; Gabel et al., 2017c; Janz et al., 2014; Kehrig et al., 2019). Longitudinal evidence supports that boys and girls who had higher levels of PA throughout childhood and into late adolescence had better bone geometry than their peers with lower levels of PA (Janz et al., 2014). This may be a concern for children with DM1, as previous study findings reported lower levels of MVPA in children with DM1 (Valerio et al., 2007). In my thesis data, however, there were no differences in daily minutes of MVPA, VPA, or number of impacts between groups. No previous studies have reported a relationship between PA and cortical pore diameter in TDC, however MVPA was identified as a positive independent predictor of total bone area and cortical porosity at the tibia, but not at the radius in TDC (Gabel et al., 2017c). It is important to also note that Gabel et al. (2017c) studied healthy adolescents, did not adjust models for site-specific muscle area, and the average entry age was about 15 years (Gabel et al., 2017c) which challenges comparison to my data. Due to limitations in statistical power to assess group-VPA interaction effects, and a limited number of studies exploring the relationship between PA and cortical micro-architecture, my thesis findings should be considered preliminary and future studies including larger sample of children and youth with DM1 are warranted.

6.3 Role of Maturity on Bone Size, Density, and Micro-Architecture

As long bones develop, it is important to consider that differences in maturity and growth-related changes in bone size, density, and micro-architecture may influence group differences in these bone outcomes in pediatric populations (Bunyamin et al., 2019; Gabel et al., 2017a). Evidence of developmental changes in HR-pQCT outcomes of bone size, density, and micro-architecture are

limited. However, our group previously reported 1-year changes at the distal radius and tibia bone in children with a mean age of 10.4y at baseline to 11.5y at follow-up (Bunyamin et al., 2019). At both sites, total bone area and density, cortical density and thickness, trabecular density and thickness increased while cortical porosity, and pore diameter declined (Bunyamin et al., 2019). These findings suggest that larger bone sizes, with a greater density and lower porosity, could be anticipated in a more mature group of children. This is important to consider, as the DM1 group was approximately 1-year older and more mature than the TDC group, and several of the group differences in bone outcomes I observed in children with DM1 may be explained by their greater maturity; despite of my attempted to control for the influence of maturity by adjusting for maturity in the models.

6.4 Low Bone Turnover in Children with DM1

Differences in bone size, density, and micro-architecture between groups may also be explained by the lower levels of bone turnover in individuals with DM1 (Hygum et al., 2017; Napoli et al., 2017). Changes at distal region of long bones during growth (including bone modeling and remodeling) are likely due to consolidation of the cortex (Bunyamin et al., 2019). This consolidation may be due to fusion of smaller trabeculae into the cortical bone (Bunyamin et al., 2019). It is possible that these structural differences observed in children with DM1, such as a lower total bone area, in the presence of a thicker cortex and lower levels of cortical porosity observed may reflect lower bone turnover. Previous findings also highlight lower levels of bone formation markers reported in children with DM1 (Chen et al., 2019; Napoli et al., 2017). Chen et al. (2019) reported a lower bone-specific alkaline phosphatase (marker of bone formation) in children with poor glycemic control, despite normal levels of circulating IGF-1 (Chen et al.,

2019). I do not suspect that lower levels of cortical porosity in children with DM1 will carry into adulthood, as previous evidence has shown that cortical porosity and pore volume were greater in adult men and women with diabetes, whereas they found no significant differences in total bone size and cortical thickness (Paccou, Ward, Jameson et al., 2016). These new observations of lower levels of cortical porosity in children with DM1 offer a stark contrast to the greater levels of cortical porosity in adults with DM1 which may serve as the basis for investigating longitudinal changes in cortical porosity from childhood to adulthood in individuals with DM1.

Based on previous associations of HR-pQCT outcomes in boys and girls with low-energy fractures, greater total BMD, cortical BMD and cortical thickness may be considered beneficial for resisting fractures (Farr, Amin, Melton et al., 2014; Määttä et al., 2015; Macdonald et al., 2018). Whereas, a lower trabecular thickness (Määttä et al., 2015), lower trabecular number, or greater trabecular separation (Farr et al., 2014) may be considered detrimental. Physiological factors inducing oxidative stress and inflammation, low levels of IGF-1 or insulin may better explain differences in bone micro-architecture in children and youth with DM1.

6.5 Role of BMI and Nutrition on Bone Size, Density, and Micro-Architecture

BMI and nutrition are important factors influencing bone outcomes in children and youth (Määttä et al., 2015; Sioen et al., 2015). It has been recommended to adjust bone comparisons for the BMI z-score in children with DM1, as they are reported to have BMIs above the 50^{th} centile for their age (Johnson, Cooper, Jones et al., 2013). BMI is a good population-based measurement of body size, and positively associated with trabecular density and trabecular number, and negatively associated with trabecular separation at the distal radius (Määttä et al., 2015).

Findings from my thesis did not agree with previous findings that children with DM1 have a higher BMI z-score than TDC (DM1 group, BMI z-score=0.53; compared to TDC group, BMI z-score=0.16, p=0.158). This may be due to a possible selection bias in our small sample of children with DM1.

Nutrition is also an important factor for achieving optimal bone growth and development. Previous literature states that skeletal growth and development is impaired at very low protein intakes (Ginty, 2003), and dairy consumption are positively associated with DXA measurements of bone mineral content and areal BMD (Sioen et al., 2015). A previous study investigating the modulating role of nutritional factors on QUS-measured bone status in children with DM1 found no differences in calcium intake and serum levels of vitamin D between children with DM1 and sex- and age-matched controls (Galluzzi, Stagi, Salti et al., 2005). To address the potential disparity in nutritional intakes between children and youth with DM1 and TDC, child participants and their parents were instructed to complete a food-frequency questionnaire as previously stated in the methods. However, there were no significant differences in daily intake of protein, calcium, or vitamin D between children with DM1 and TDC.

6.6 Strengths and Limitations

There are definite strengths and limitations of my thesis that are important to discuss. The main strengths of my thesis include the tools I used to measure bone size, density, and micro-architecture and record physical activity. First, HR-pQCT is an excellent tool for assessing populations at a higher risk of obtaining a bone fracture, as previous studies have found that cortical and trabecular micro-architecture outcomes, measured using HR-pQCT, are associated

with fracture risk in older adults independent of aBMD (Samelson et al., 2019), which is the current clinical method used to predict fracture risk. The short-term precision and reliability of HR-pQCT for use in child populations has also been assessed (Bunyamin et al., 2019; Kawalilak et al., 2017). Second, the accelerometers used in this study have been validated for objectively-measuring different intensities of physical activity in children and youth (Evenson et al., 2008; Trost et al., 2011) and have been previously used to assess impact counts in children (Kehrig et al., 2019). Both of these tools offer substantial improvements to tools used in other studies, namely DXA and self-reported physical activity questionnaires (Maggio et al., 2012).

The limitations of my findings including the cross-sectional design, a small sample size of children with DM1, a difference in maturity between groups, and the potential for a selection bias in our sample of children and youth with DM1. First, I used a cross-sectional design to address my objectives. As a result, I was unable to observe changes in bone size, density, and micro-architecture during growth, as that may have yielded important evidence. I was also unable to causatively link bone micro-architecture and PA using a cross-sectional design. Instead, I was only able to identify VPA as an independent factor influencing cortical pore diameter in a pooled sample of children with DM1 and TDC. Second, I had a small sample size of children with DM1 (n=21). Therefore, I was unable to assess group-sex or group-PA interactions, run sex-specific analyses, or control for other variables such as length of DM1 diagnosis, nutritional or hormone factors. Third, the DM1 group was more mature than the TDC group. I adjusted for the difference in maturity in my analyses, however this may have been better addressed through case-control matching in a larger sample. This would have eliminated the difference in maturity between groups. Fourth, there is the potential for a selection bias in our cohort of children and youth with DM1, as these children were recruited from diabetes clinics,

diabetes camps, and diabetes family days which may cater to children from families of a higher socioeconomic status. Since socioeconomic status was not measured, there is the potential that these recruitment venues did not allow for the inclusion of a representative sample of children from families with a low socioeconomic status, which has been shown to be associated with poorer glycemic control in children with DM1 (Hassan, Loar, Anderson et al., 2006).

6.7 Directions for Future Research

Since we are assessing children, we can gain valuable insight into how DM1 may adversely affect bone development using evidence from change data. My thesis offers a good basis of support that may be used to guide researchers assessing longitudinal changes in total, cortical, and trabecular area, density, and micro-architecture development in children with DM1 followed into adulthood and an RCT assessing the effectiveness of a vigorous intensity PA program on children with DM1. Future researchers may also want to consider the roles of hyperglycaemia, oxidative stress, AGEs, marrow composition, inflammatory factors and adipokines, and the lower activation frequency of bone remodelling units on bone in people with DM1 (Chen et al., 2019; Napoli et al., 2017). For the RCT assessing the efficacy of a VPA on bone size, density, and micro-architecture, researchers may choose to recruit children and youth with DM1 and TDC into their study and randomize them into a vigorous PA exercise group or light PA group (control group); for a total of 4 groups. It would be important for researchers to track the duration and intensity of physical activity using an objective tool, such as an accelerometer during the intervention sessions. Baseline and follow-up measurements could include HR-pQCT assessment of bone density and micro-architecture at the radius and tibia, pQCT muscle area, and questionnaires to gather information of health and nutrition, similar to the tools used in my

thesis. Additionally, researchers may want to consider tracking potential mediators of bone micro-architecture in children with DM1 such as: daily blood glucose levels (hyperglycaemia), markers of oxidative stress, AGEs, inflammation, marrow adiposity, IGF-1, and insulin. This study would help us to determine how bone micro-architecture develops in children with DM1, if VPA is effective at improving bone micro-architecture, and if these various physiological factors underpin the high fracture rates in children with DM1.

7 CONCLUSIONS

7.1 Conclusions of Primary Objective

This thesis is the first to provide evidence of the differences, particularly in cortical bone micro-architecture between children and youth with DM1 and TDC. Children and youth with DM1 had observed deficits total bone area, alongside a greater total BMD, cortical BMD, and cortical thickness, and a lower cortical porosity, pore volume, pore diameter, trabecular area, trabecular number, and a greater trabecular separation at the radius. Lower cortical porosity, pore volume, and pore diameter was also observed the tibia.

7.2 Conclusions of Secondary Objective

My thesis also provides preliminary evidence that daily minutes of VPA may play an independent role predicting the variance in cortical bone micro-architecture in a mixed-cohort of children and youth with DM1 and TDC. However, it is likely that VPA only plays a minor role in explaining these group differences, as adjusting for VPA contributed ≤1.2% change in group

differences in total, cortical, and trabecular area, density, and micro-architecture outcomes compared to the base model at the radius.

REFERENCES

Al Nazer, R., Lanovaz, J., Kawalilak, C., Johnston, J. D., & Kontulainen, S. (2012). Direct in vivo strain measurements in human bone-a systematic literature review. *J. Biomech., 45*(1), 27-40.

Baroncelli, G. I. (2008). Quantitative ultrasound methods to assess bone mineral status in children: technical characteristics, performance, and clinical application. *Pediatr Res, 63*(3), 220-228.

Bechtold, S., Putzker, S., Bonfig, W., Fuchs, O., Dirlenbach, I., & Schwarz, H. P. (2007). Bone size normalizes with age in children and adolescents with type 1 diabetes. *Diabetes Care, 30*(8), 2046-2050.

Binkley, T. L., Berry, R., & Specker, B. L. (2008). Methods for measurement of pediatric bone. *Rev Endocr Metab Disord, 9*(2), 95-106.

Björkman, K., Duff, W. R. D., Frank-Wilson, A., Kehrig, A. M., Johnston, J. D., & Kontulainen, S. (2017). Peripheral quantitative computed tomography imaged measures of muscle area and density at the forearm and lower leg of children are precise with errors ranging between 1-4%. *J Musculoskelet Neuronal Interact, 17*(4), 352.

Bolotin, H. H., & Sievanen, H. (2001). Inaccuracies inherent in dual-energy X-ray absorptiometry in vivo bone mineral density can seriously mislead diagnostic/prognostic interpretations of patient-specific bone fragility. *J Bone Miner Res, 16*(5), 799-805.

Boucher, B., Cotterchio, M., Kreiger, N., Nadalin, V., Block, T., & Block, G. (2006). Validity and reliability of the Block98 food-frequency questionnaire in a sample of Canadian women. *Public Health Nutr, 9*(1), 84-93.

Boyd, S. K. (2008). Site-specific variation of bone micro-architecture in the distal radius and tibia. *J Clin Densitom, 11*(3), 424-430.

Bunyamin, A., Bjorkman, K., Kawalilak, C., Hosseinitabatabaei, S., Teare, A., Johnston, J., & Kontulainen, S. (2019). Reliability of annual changes and monitoring time intervals for bone strength, size, density, and microarchitectural development at the distal radius and tibia in children: A 1-year HR-pQCT follow-up. *J Bone Miner Res, 34*(7), 1297-1305.

Burghardt, A. J., Issever, A. S., Schwartz, A. V., Davis, K. A., Masharani, U., Majumdar, S., & Link, T. M. (2010). High-resolution peripheral quantitative computed tomographic

imaging of cortical and trabecular bone microarchitecture in patients with type 2 diabetes mellitus. *J Clin Endocrinol Metab, 95*(11), 5045-5055.

Burrows, M., Liu, D., Moore, S., & McKay, H. (2010). Bone microstructure at the distal tibia provides a strength advantage to males in late puberty: an HR-pQCT study. *J Bone Miner Res, 25*(6), 1423-1432.

Chen, S. C., Shepherd, S., McMillan, M., McNeilly, J., Foster, J., Wong, S. C., Robertson, K. J., & Ahmed, S. F. (2019). Skeletal fragility & its clinical determinants in children with type 1 diabetes. *J Clin Endocrinol Metab, 104*(8), 3585-3594.

Chevalley, T., Bonjour, J. P., van Rietbergen, B., Ferrari, S., & Rizzoli, R. (2011). Fractures during childhood and adolescence in healthy boys: relation with bone mass, microstructure, and strength. *J Clin Endocrinol Metab, 96*(10), 3134-3142.

Choi, L., Liu, Z., Matthews, C. E., & Buchowski, M. S. (2011). Validation of accelerometer wear and nonwear time classification algorithm. *Med Sci Sports Exerc, 43*(2), 357-364.

Cummings, S. R., Bates, D., & Black, D. M. (2002). Clinical use of bone densitometry: Scientific review. *JAMA, 288*(15), 1889-1897.

de Lima, V. A., Mascarenhas, L. P. G., Decimo, J. P., de Souza, W. C., Monteiro, A. L. S., Lahart, I., Franca, S. N., & Leite, N. (2017). Physical activity levels of adolescents with type 1 diabetes physical activity in T1D. *Pediatr Exerc Sci, 29*(2), 213-219.

Duff, W. R. D., Björkman, K. M., Kawalilak, C. E., Kehrig, A. M., Wiebe, S., & Kontulainen, S. (2017). Precision of pQCT-measured total, trabecular and cortical bone area, content, density and estimated bone strength in children. *J Musculoskelet Neuronal Interact, 17*(2), 59-68.

Evenson, K. R., Catellier, D. J., Gill, K., Ondrak, K. S., & McMurray, R. G. (2008). Calibration of two objective measures of physical activity for children. *J Sports Sci, 26*(14), 1557-1565.

Farlay, D., Armas, L. A., Gineyts, E., Akhter, M. P., Recker, R. R., & Boivin, G. (2016). Nonenzymatic glycation and degree of mineralization are higher in bone from fractured patients with type 1 diabetes mellitus. *J Bone Miner Res, 31*(1), 190-195.

Farr, J. N., Amin, S., Melton, L. J., Kirmani, S., McCready, L. K., Atkinson, E. J., Müller, R., & Khosla, S. (2014). Bone strength and structural deficits in children and adolescents with a distal forearm fracture resulting from mild trauma. *J Bone Miner Res, 29*(3), 590-599.

Franceschi, R., Longhi, S., Cauvin, V., Fassio, A., Gallo, G., Lupi, F., Reinstadler, P., Fanolla, A., Gatti, D., & Radetti, G. (2017). Bone geometry, quality, and bone markers in children with type 1 diabetes mellitus. *Calcif Tissue Int, 102*(6), 657-665.

Frost, H. M. (1987). Bone "mass" and the "mechanostat": A proposal. *Anat Rec, 219*(1), 1-9.

Gabel, L., Macdonald, H. M., & McKay, H. A. (2017a). Sex differences and growth-related adaptations in bone microarchitecture, geometry, density, and strength from childhood to early adulthood: A mixed longitudinal HR-pQCT study. *J Bone Miner Res, 32*(2), 250-263.

Gabel, L., Macdonald, H. M., Nettlefold, L., & McKay, H. A. (2017b). Bouts of vigorous physical activity and bone strength accrual during adolescence. *Pediatr Exerc Sci, 29*(4), 465-475.

Gabel, L., Macdonald, H. M., Nettlefold, L., & McKay, H. A. (2017c). Physical activity, sedentary time, and bone strength from childhood to early adulthood: A mixed longitudinal HR-pQCT study. *J Bone Miner Res, 32*(7), 1525-1536.

Galluzzi, F., Stagi, S., Salti, R., Toni, S., Piscitelli, E., Simonini, G., Falcini, F., & Chiarelli, F. (2005). Osteoprotegerin serum levels in children with type 1 diabetes: a potential modulating role in bone status. *Eur J Endocrinol, 153*(6), 879-885.

Garcia-Hernandez, A., Arzate, H., Gil-Chavarria, I., Rojo, R., & Moreno-Fierros, L. (2012). High glucose concentrations alter the biomineralization process in human osteoblastic cells. *Bone, 50*(1), 276-288.

Ginty, F. (2003). Dietary protein and bone health. *Proc Nutr Soc, 62*(4), 867-876.

Hassan, K., Loar, R., Anderson, B. J., & Heptulla, R. A. (2006). The role of socioeconomic status, depression, quality of life, and glycemic control in type 1 diabetes mellitus. *J Pediatr, 149*(4), 526-531.

Heap, J., Murray, M. A., Miller, S. C., Jalili, T., & Moyer-Mileur, L. J. (2004). Alterations in bone characteristics associated with glycemic control in adolescents with type 1 diabetes mellitus. *J Pediatr, 144*(1), 56-62.

Hygum, K., Starup-Linde, J., Harslof, T., Vestergaard, P., & Langdahl, B. L. (2017). Mechanisms in endocrinology: Diabetes mellitus, a state of low bone turnover - A systematic review and meta-analysis. *Eur J Endocrinol, 176*(3), R137-157.

Janz, K. F., Letuchy, E. M., Burns, T. L., Eichenberger Gilmore, J. M., Torner, J. C., & Levy, S. M. (2014). Objectively measured physical activity trajectories predict adolescent bone strength: Iowa bone development study. *Br J Sports Med, 48*(13), 1032-1036.

Johnson, S. R., Cooper, M. N., Jones, T. W., & Davis, E. A. (2013). Long-term outcome of insulin pump therapy in children with type 1 diabetes assessed in a large population-based case-control study. *Diabetologia, 56*(11), 2392-2400.

Kawalilak, C. E., Bunyamin, A. T., Bjorkman, K. M., Johnston, J. D., & Kontulainen, S. A. (2017). Precision of bone density and micro-architectural properties at the distal radius and tibia in children: An HR-pQCT study. *Osteoporos Int, 28*(11), 3189-3197.

Kehrig, A. M., Bjorkman, K., Muhajarine, N., Johnston, J. D., & Kontulainen, S. A. (2018). Moderate to vigorous physical activity and impact loading independently predict variance in bone strength at the tibia but not at the radius in children. *Appl. Physiol. Nutr. Metab.*

Kehrig, A. M., Bjorkman, K. M., Muhajarine, N., Johnston, J. D., & Kontulainen, S. A. (2019). Moderate to vigorous physical activity and impact loading independently predict variance in bone strength at the tibia but not at the radius in children. *Appl Physiol Nutr Metab, 44*(3), 326-331.

Kontulainen, S. A., Johnston, J. D., Liu, D., Leung, C., Oxland, T. R., & McKay, H. A. (2008). Strength indices from pQCT imaging predict up to 85% of variance in bone failure properties at tibial epiphysis and diaphysis. *J Musculoskelet Neuronal Interact, 8*(4), 401-409.

Kontulainen, S. A., Kawalilak, C. E., Johnston, J. D., & Bailey, D. A. (2013). Prevention of osteoporosis and bone fragility: A pediatric concern. *AJLM, 7*(6), 405-417.

Kuczmarski, R. J., Ogden, C. L., Grummer-Strawn, L. M., Flegal, K. M., Guo, S. S., Wei, R., Mei, Z., Curtin, L. R., Roche, A. F., & Johnson, C. L. (2000). CDC growth charts: United States. *Adv Data*, (314), 1-27.

Laib, A., & Ruegsegger, P. (1999). Calibration of trabecular bone structure measurements of in vivo three-dimensional peripheral quantitative computed tomography with 28-micron-resolution microcomputed tomography. *Bone, 24*(1), 35-39.

Lettgen, B., Hauffa, B., Mohlmann, C., Jeken, C., & Reiners, C. (1995). Bone mineral density in children and adolescents with juvenile diabetes: Selective measurement of bone mineral

density of trabecular and cortical bone using peripheral quantitative computed tomography. *Horm Res, 43*(5), 173-175.

Liu, D., Burrows, M., Egeli, D., & McKay, H. (2010). Site specificity of bone architecture between the distal radius and distal tibia in children and adolescents: An HR-pQCT study. *Calcif Tissue Int, 87*(4), 314-323.

Liu, X. S., Zhang, X. H., Sekhon, K. K., Adams, M. F., McMahon, D. J., Bilezikian, J. P., Shane, E., & Guo, X. E. (2010). High-resolution peripheral quantitative computed tomography can assess microstructural and mechanical properties of human distal tibial bone. *J Bone Miner Res, 25*(4), 746-756.

Määttä, M., Macdonald, H. M., Mulpuri, K., & McKay, H. A. (2015). Deficits in distal radius bone strength, density and microstructure are associated with forearm fractures in girls: an HR-pQCT study. *Osteoporos Int, 26*(3), 1163-1174.

Macdonald, H. M., Maatta, M., Gabel, L., Mulpuri, K., & McKay, H. A. (2018). Bone strength in girls and boys after a distal radius fracture: A 2-year HR-pQCT double cohort study. *J Bone Miner Res, 33*(2), 229-240.

Maggio, A. B., Rizzoli, R. R., Marchand, L. M., Ferrari, S., Beghetti, M., & Farpour-Lambert, N. J. (2012). Physical activity increases bone mineral density in children with type 1 diabetes. *Med Sci Sports Exerc, 44*(7), 1206-1211.

Majumdar, S., Genant, H. K., Grampp, S., Newitt, D. C., Truong, V. H., Lin, J. C., & Mathur, A. (1997). Correlation of trabecular bone structure with age, bone mineral density, and osteoporotic status: In vivo studies in the distal radius using high resolution magnetic resonance imaging. *J Bone Miner Res, 12*(1), 111-118.

Maratova, K., Soucek, O., Matyskova, J., Hlavka, Z., Petruzelkova, L., Obermannova, B., Pruhova, S., Kolouskova, S., & Sumnik, Z. (2018). Muscle functions and bone strength are impaired in adolescents with type 1 diabetes. *Bone, 106*, 22-27.

Meyer, U., Ernst, D., Schott, S., Riera, C., Hattendorf, J., Romkes, J., Granacher, U., Gopfert, B., & Kriemler, S. (2015). Validation of two accelerometers to determine mechanical loading of physical activities in children. *J Sports Sci, 33*(16), 1702-1709.

Michaliszyn, S. F., & Faulkner, M. S. (2010). Physical activity and sedentary behavior in adolescents with type 1 diabetes. *Res Nurs Health, 33*(5), 441-449.

Migueles, J. H., Cadenas-Sanchez, C., Ekelund, U., Delisle Nystrom, C., Mora-Gonzalez, J., Lof, M., Labayen, I., Ruiz, J. R., & Ortega, F. B. (2017). Accelerometer data collection and processing criteria to assess physical activity and other outcomes: A systematic review and practical considerations. *Sports Med, 47*(9), 1821-1845.

Mokawem, M., & Scott, B. (2015). Children's forearm fractures. *J Orthop, 29*(1), 57-68.

Moore, S. A., McKay, H. A., Macdonald, H., Nettlefold, L., Baxter-Jones, A. D., Cameron, N., & Brasher, P. M. (2015). Enhancing a somatic maturity prediction model. *Med Sci Sports Exerc, 47*(8), 1755-1764.

Moyer-Mileur, L. J., Dixon, S. B., Quick, J. L., Askew, E. W., & Murray, M. A. (2004). Bone mineral acquisition in adolescents with type 1 diabetes. *J Pediatr, 145*(5), 662-669.

Muller, M., Mitton, D., Moilanen, P., Bousson, V., Talmant, M., & Laugier, P. (2008). Prediction of bone mechanical properties using QUS and pQCT: Study of the human distal radius. *Med Eng Phys, 30*(6), 761-767.

Napoli, N., Chandran, M., Pierroz, D. D., Abrahamsen, B., Schwartz, A. V., & Ferrari, S. L. (2017). Mechanisms of diabetes mellitus-induced bone fragility. *Nat Rev Endocrinol, 13*(4), 208-219.

National Osteoporosis Society. (2004). A practical guide to bone densitometry in children. *National Osteoporosis Society*, Camerton, Bath, UK.

Nishiyama, K. K., Macdonald, H. M., Moore, S. A., Fung, T., Boyd, S. K., & McKay, H. A. (2012). Cortical porosity is higher in boys compared with girls at the distal radius and distal tibia during pubertal growth: an HR-pQCT study. *J Bone Miner Res, 27*(2), 273-282.

Paccou, J., Ward, K. A., Jameson, K. A., Dennison, E. M., Cooper, C., & Edwards, M. H. (2016). Bone microarchitecture in men and women with diabetes: The importance of cortical porosity. *Calcif Tissue Int, 98*(5), 465-473.

Parajuli, A., Liu, C., Li, W., Gu, X., Lai, X., Pei, S., Price, C., You, L., Lu, X. L., & Wang, L. (2015). Bone's responses to mechanical loading are impaired in type 1 diabetes. *Bone, 81*, 152-160.

Patsch, J. M., Burghardt, A. J., Kazakia, G., & Majumdar, S. (2011). Noninvasive imaging of bone microarchitecture. *Ann N Y Acad Sci, 1240*, 77-87.

Pialat, J. B., Burghardt, A. J., Sode, M., Link, T. M., & Majumdar, S. (2012). Visual grading of motion induced image degradation in high resolution peripheral computed tomography: Impact of image quality on measures of bone density and micro-architecture. *Bone, 50*(1), 111-118.

Roggen, I., Gies, I., Vanbesien, J., Louis, O., & De Schepper, J. (2013). Trabecular bone mineral density and bone geometry of the distal radius at completion of pubertal growth in childhood type 1 diabetes. *Horm Res Paediatr, 79*(2), 68-74.

Saha, M. T., Sievanen, H., Salo, M. K., Tulokas, S., & Saha, H. H. (2009). Bone mass and structure in adolescents with type 1 diabetes compared to healthy peers. *Osteoporos Int, 20*(8), 1401-1406.

Samelson, E. J., Broe, K. E., Xu, H., Yang, L., Boyd, S., Biver, E., Szulc, P., Adachi, J., Amin, S., Atkinson, E., Berger, C., Burt, L., Chapurlat, R., Chevalley, T., Ferrari, S., Goltzman, D., Hanley, D. A., Hannan, M. T., Khosla, S., Liu, C. T., Lorentzon, M., Mellstrom, D., Merle, B., Nethander, M., Rizzoli, R., Sornay-Rendu, E., Van Rietbergen, B., Sundh, D., Wong, A. K. O., Ohlsson, C., Demissie, S., Kiel, D. P., & Bouxsein, M. L. (2019). Cortical and trabecular bone microarchitecture as an independent predictor of incident fracture risk in older women and men in the Bone Microarchitecture International Consortium (BoMIC): A prospective study. *Lancet Diabetes Endocrinol, 7*(1), 34-43.

Schoenau, E., & Frost, H. M. (2002). The "muscle-bone unit" in children and adolescents. *Calcif Tissue Int, 70*(5), 405-407.

Shmueli, G. (2010). To explain or to predict? *Stat Sci, 25*(3), 289-310.

Sioen, I., Michels, N., Polfliet, C., De Smet, S., D'Haese, S., Roggen, I., Deschepper, J., Goemaere, S., Valtuena, J., & De Henauw, S. (2015). The influence of dairy consumption, sedentary behaviour and physical activity on bone mass in Flemish children: A cross-sectional study. *BMC Public Health, 15*(1), 717.

Trost, S. G., Loprinzi, P. D., Moore, R., & Pfeiffer, K. A. (2011). Comparison of accelerometer cut points for predicting activity intensity in youth. *Med Sci Sports Exerc, 43*(7), 1360-1368.

Turner, C. H., & Robling, A. G. (2003). Designing exercise regimens to increase bone strength. *Exerc Sport Sci Rev, 31*(1), 45-50.

Valerio, G., Spagnuolo, M. I., Lombardi, F., Spadaro, R., Siano, M., & Franzese, A. (2007). Physical activity and sports participation in children and adolescents with type 1 diabetes mellitus. *Nutr Metab Cardiovasc Dis, 17*(5), 376-382.

Weber, D. R., Gordon, R. J., Kelley, J. C., Leonard, M. B., Willi, S. M., Hatch-Stein, J., Kelly, A., Kosacci, O., Kucheruk, O., Kaafarani, M., & Zemel, B. S. (2019). Poor glycemic control is associated with impaired bone accrual in the year following a diagnosis of type 1 diabetes. *J Clin Endocrinol Metab, 104*(10), 4511-4520.

Weber, D. R., Haynes, K., Leonard, M. B., Willi, S. M., & Denburg, M. R. (2015). Type 1 diabetes is associated with an increased risk of fracture across the life span: A population-based cohort study using The Health Improvement Network (THIN). *Diabetes Care, 38*(10), 1913-1920.

APPENDIX

To address potential errors in my results that may be due to variables that failed to meet the assumptions of normality and homogeneity of variances, I opted to re-run my analyses after applying a natural log transformation to the variables that did not meet these assumptions. Variables in my models that failed to meet the assumption of normality include: daily minutes of VPA, daily impacts, Tb.Sp.SD, Ct.Ar, Ct.TV, Ct.BV, apparent Ct.Th, Fine Ct.Th at the radius, and Ct.TMD, apparent Ct.Th, and fine Ct.Th at the tibia. Variables that failed to meet the assumption of homogeneity of variance include, apparent Ct.Th and Co.Po at the radius. After applying natural log transformations to the variables above, I re-tested assumptions and re-ran analyses for my primary and secondary objectives. All transformed variables now met the assumptions of normality and homogeneity of variances.

For my primary objective, I found significant differences in bone size, density, and cortical and trabecular micro-architecture radius (F=7.61, p<0.001) and significant differences in cortical micro-architecture at the tibia (F=3.01, p=0.002) between children and youth with DM1 and TDC. At the radius, children with DM1 had a lower total bone area, greater total BMD, cortical BMD, cortical TMD, apparent cortical thickness, fine cortical thickness; lower cortical porosity, pore volume, pore diameter, trabecular area, trabecular number; and greater trabecular separation (Table 7). At the tibia, children with DM1 had a lower cortical porosity, pore volume, and pore diameter (Table 8).

Table 7. Descriptive statistics and adjusted[†] group differences in bone size, density, and micro-architecture at the radius between children and youth with type 1 diabetes (DM1) and typically developing children and youth (TDC) after log transformations.

	DM1 (n=20)		TDC (n=45)					
	Mean	SD	Mean	SD	*Adj Mean Diff	*95% CI of Adj Diff		*p-value
						Lower	Upper	

Tt.Ar (mm²)	193.3	43.3	208.4	41.0	**-28.3**	**-44.4**	**-12.1**	**0.001**
Tt.BMD (mg HA/cm³)	277.9	46.1	246.8	40.7	**30.4**	**8.7**	**52.0**	**0.007**
ln(Ct.Ar)	3.68	0.29	3.67	0.18	-0.03	-0.12	0.06	0.488
ln(Ct.TV)	5.88	0.29	5.87	0.18	-0.03	-0.12	0.06	0.488
ln(Ct.BV)	5.77	0.32	5.63	0.18	0.08	-0.01	0.18	0.097
Ct.BMD (mg HA/cm³)	771.0	62.8	690.5	52.4	**65.0**	**37.4**	**92.6**	**<0.001**
Ct.TMD (mg HA/cm³)	811.8	55.1	762.6	35.3	**35.7**	**15.0**	**56.3**	**0.001**
ln(Apparent Ct.Th)	-0.31	0.27	-0.54	0.17	**0.19**	**0.08**	**0.29**	**0.001**
ln(Fine Ct.Th)	-0.72	0.22	-0.96	0.14	**0.20**	**0.11**	**0.29**	**<0.001**
ln(Ct.Po)	-3.3	0.5	-2.6	0.3	**-0.5**	**-0.7**	**-0.3**	**<0.001**
Ct.Po.V (mm³)	14.3	8.4	23.0	11.8	**-7.6**	**-12.6**	**-2.6**	**0.004**
Ct.Po.Dm (µm)	143	7.1	162	9.9	**-17**	**-22**	**-12.9**	**<0.001**
Tb.Ar (mm²)	154.8	37.5	177.4	38.8	**-32.9**	**-49.9**	**-15.9**	**<0.001**
Tb.BMD (mg HA/cm³)	166.0	28.8	179.1	34.4	-7.8	-23.5	7.9	0.323
BV/TV (%)	13.8	2.4	14.9	2.9	-0.7	-2.0	0.7	0.322
Tb.N (1/mm)	2.1	0.2	2.3	0.2	**-0.1**	**-0.3**	**0.0**	**0.028**
Tb.Th (µm)	66	8.7	66	9.7	1	-3.5	6.0	0.606
Tb.Sp (µm)	416	51.4	381	51.0	**27**	**0.7**	**53.7**	**0.044**
ln(Tb.Sp.SD)	-1.83	0.16	-1.94	0.21	0.07	-0.03	0.17	0.145

Abbreviations: Tt.Ar = total bone area, Tt.BMD = total bone mineral density, Ct.Ar = cortical area, Ct.TV = cortical total volume, Ct.BV = cortical bone volume, Ct.BMD = cortical bone mineral density, Ct.TMD = cortical tissue mineral density, Ct.Th = cortical thickness, Ct.Po = cortical porosity, Ct.Po.V = cortical pore volume, Ct.Po.Dm = cortical pore diameter, Tb.Ar = trabecular area, Tb.BMD = trabecular bone mineral density, BV/TV = trabecular bone volume fraction, Tb.N = trabecular number, Tb.Th = trabecular thickness, Tb.Sp = trabecular separation, Tb.Sp.SD = trabecular heterogeneity. *Bonferroni adjustment for multiple comparisons. †Covariates are evaluated as sex (girls=1, boys=2), years from age at PHV = -1.17y, forearm muscle area = 2327.4 mm², and BMI z-score = 0.27.
ln(x) = natural log transformation

Table 8. Descriptive statistics and adjusted† group differences in bone size, density, and micro-architecture at the tibia between children and youth with type 1 diabetes (DM1) and typically developing children and youth (TDC) after log transformations.

	DM1 (n=20)		TDC (n=45)					
	Mean	SD	Mean	SD	*Adj Mean Diff	*95% CI of Adj Diff		*p-value
						Lower	Upper	
Tt.Ar (mm²)	682.3	107.0	673.4	115.3	-40.6	-89.8	8.7	0.104
Tt.BMD (mg HA/cm³)	239.3	32.5	236.4	31.6	-0.8	-18.4	16.9	0.930
Ct.Ar (mm²)	80.3	20.2	78.9	16.5	-7.1	-15.2	1.1	0.088
Ct.TV (mm³)	723.9	182.3	711.9	149.2	-63.8	-137.5	9.8	0.088
Ct.BV (mm³)	629.9	176.7	585.8	128.7	-30.2	-96.1	35.8	0.364
Ct.BMD (mg HA/cm³)	757.3	73.6	719.1	42.0	14.4	-15.1	43.9	0.333
ln(Ct.TMD)	6.70	0.08	6.67	0.04	0.00	-0.03	0.03	0.988
ln(Apparent Ct.Th)	-0.31	0.24	-0.40	0.22	0.00	-0.12	0.12	0.981
ln(Fine Ct.Th)	-0.85	0.19	-0.95	0.12	0.05	-0.04	0.13	0.267
Ct.Po (%)	6.1	2.3	8.0	2.5	**-1.8**	**-3.2**	**-0.3**	**0.018**
Ct.Po.V (mm³)	40.4	17.8	52.0	23.8	**-15.1**	**-27.6**	**-2.6**	**0.018**
Ct.Po.Dm (µm)	152	7.9	163	9.2	**-11**	**-15.8**	**-5.4**	**<0.001**
Tb.Ar (mm²)	607.9	96.4	601.5	111.3	-41.1	-90.5	8.2	0.101
Tb.BMD (mg HA/cm³)	180.4	19.0	187.5	24.4	-5.3	-18.4	7.8	0.422
BV/TV (%)	15.0	1.6	15.6	2.0	-0.4	-1.5	0.6	0.414
Tb.N (1/mm)	2.1	0.2	2.1	0.3	0.0	-0.1	0.1	0.964

Tb.Th (μm)	74	9.5	76	11.5	-3	-9.0	3.3	0.353
Tb.Sp (μm)	416	42.7	412	61.3	-2	-33.1	29.2	0.901
Tb.Sp.SD (μm)	174	30.8	170	37.5	-2	-21.5	17.2	0.822

Abbreviations: Tt.Ar = total bone area, Tt.BMD = total bone mineral density, Ct.Ar = cortical area, Ct.TV = cortical total volume, Ct.BV = cortical bone volume, Ct.BMD = cortical bone mineral density, Ct.TMD = cortical tissue mineral density, Ct.Th = cortical thickness, Ct.Po = cortical porosity, Ct.Po.V = cortical pore volume, Ct.Po.Dm = cortical pore diameter, Tb.Ar = trabecular area, Tb.BMD = trabecular bone mineral density, BV/TV = trabecular bone volume fraction, Tb.N = trabecular number, Tb.Th = trabecular thickness, Tb.Sp = trabecular separation, Tb.Sp.SD = trabecular heterogeneity. *Bonferroni adjustment for multiple comparisons.
†Covariates were evaluated as sex (girls=1, boys=2), years from age at PHV = -1.10y, lower leg muscle area = 4519.9mm², and BMI z-score = 0.27.
ln(x) = natural log transformation.

For my secondary objective, daily minutes of VPA independently predicted the variance in cortical TMD (Std. β=-0.21, p=0.041), fine cortical thickness (Std. β=-0.24, p=0.024), and cortical pore diameter at the radius (Std. β=-0.20, p=0.019), but did not independently predict the variance in total bone area, total or cortical BMD, apparent cortical thickness, cortical porosity, pore volume, trabecular area, number, or separation (Table 9). Daily minutes of MVPA and daily impacts did not contribute to the overall variance in bone size, density, and micro-architecture at the radius or tibia. Pairwise comparisons revealed that group differences in radius bone size, density, cortical and trabecular micro-architecture between children with DM1 and TDC remained after adjusting for daily minutes of VPA, excluding trabecular separation (p=0.053) (Table 10). After adjusting for VPA, children with DM1 still had a lower total bone area; greater total BMD, cortical BMD, cortical TMD, apparent cortical thickness, fine cortical thickness; and a lower cortical porosity, pore volume, pore diameter, trabecular area, and number at the radius (Table 10).

Table 9. Standardized β-coefficients of base model covariates and daily minutes of vigorous physical activity (VPA) for bone size, density, and micro-architecture at the radius in a pooled sample of children and youth with type 1 diabetes (DM1) and typically developing children and youth (TDC) after log transformations.

		Std. β	*p*-value
Tt.Ar	Sex	0.26	0.040
	Maturity (years from aPHV)	0.58	<0.001
	Forearm muscle area	0.31	0.060

	Body mass index z-score	0.01	0.919
	ln(Daily VPA)	0.15	0.099
	Group (DM1 and TDC)	-0.30	0.001
Tt.BMD	Sex	-0.02	0.907
	Maturity (years from aPHV)	-0.26	0.196
	Forearm muscle area	0.55	0.011
	Body mass index z-score	-0.02	0.883
	ln(Daily VPA)	-0.04	0.703
	Group (DM1 and TDC)	0.31	0.008
Ct.BMD	Sex	0.20	0.141
	Maturity (years from aPHV)	0.46	0.008
	Forearm muscle area	-0.39	0.031
	Body mass index z-score	0.50	<0.001
	ln(Daily VPA)	-0.09	0.345
	Group (DM1 and TDC)	0.44	<0.001
Ct.TMD	Sex	0.19	0.168
	Maturity (years from aPHV)	0.52	0.004
	Forearm muscle area	-0.25	0.177
	Body mass index z-score	0.38	0.004
	ln(Daily VPA)	**-0.21**	**0.041**
	Group (DM1 and TDC)	0.33	0.001
ln(Apparent Ct.Th)	Sex	0.15	0.304
	Maturity (years from aPHV)	0.25	0.184
	Forearm muscle area	0.19	0.326
	Body mass index z-score	0.01	0.934
	ln(Daily VPA)	-0.20	0.070
	Group (DM1 and TDC)	0.36	0.001
ln(Fine Ct.Th)	Sex	0.16	0.265
	Maturity (years from aPHV)	0.46	0.010
	Forearm muscle area	-0.31	0.099
	Body mass index z-score	0.25	0.059
	ln(Daily VPA)	**-0.24**	**0.024**
	Group (DM1 and TDC)	0.44	<0.001
ln(Ct.Po)	Sex	-0.10	0.444
	Maturity (years from aPHV)	-0.47	0.005
	Forearm muscle area	0.67	<0.001
	Body mass index z-score	-0.50	<0.001
	ln(Daily VPA)	0.07	0.476
	Group (DM1 and TDC)	-0.52	<0.001
Ct.Po.V	Sex	-0.10	0.510
	Maturity (years from aPHV)	-0.47	0.011
	Forearm muscle area	0.96	<0.001
	Body mass index z-score	-0.48	0.001
	ln(Daily VPA)	0.01	0.945
	Group (DM1 and TDC)	-0.31	0.004
Ct.Po.Dm	Sex	-0.02	0.865
	Maturity (years from aPHV)	-0.10	0.476
	Forearm muscle area	0.34	0.025
	Body mass index z-score	-0.56	<0.001
	ln(Daily VPA)	**-0.20**	**0.019**
	Group (DM1 and TDC)	-0.66	<0.001
Tb.Ar	Sex	0.22	0.124
	Maturity (years from aPHV)	0.49	0.005
	Forearm muscle area	0.29	0.120

	Body mass index z-score	-0.03	0.831
	ln(Daily VPA)	0.18	0.078
	Group (DM1 and TDC)	-0.37	<0.001
Tb.N	Sex	-0.36	0.032
	Maturity (years from aPHV)	-0.69	0.001
	Forearm muscle area	0.66	0.004
	Body mass index z-score	-0.12	0.452
	ln(Daily VPA)	0.06	0.595
	Group (DM1 and TDC)	-0.26	0.033
Tb.Sp	Sex	0.33	0.045
	Maturity (years from aPHV)	0.72	0.001
	Forearm muscle area	-0.73	0.001
	Body mass index z-score	0.15	0.326
	ln(Daily VPA)	-0.10	0.406
	Group (DM1 and TDC)	0.23	0.053

Abbreviations: Tt.Ar = total bone area, Tt.BMD = total bone mineral density, Ct.Ar = cortical area, Ct.TV = cortical total volume, Ct.BV = cortical bone volume, Ct.BMD = cortical bone mineral density, Ct.TMD = cortical tissue mineral density, Ct.Th = cortical thickness, Ct.Po = cortical porosity, Ct.Po.V = cortical pore volume, Ct.Po.Dm = cortical pore diameter, Tb.Ar = trabecular area, Tb.BMD = trabecular bone mineral density, BV/TV = trabecular bone volume fraction, Tb.N = trabecular number, Tb.Th = trabecular thickness, Tb.Sp = trabecular separation, Tb.Sp.SD = trabecular heterogeneity. ln(x) = natural log transformation.

Table 10. Descriptive statistics of bone size, density, and micro-architecture at the radius between children and youth with type 1 diabetes (DM1) and typically developing children and youth (TDC). Adjusting† for covariates in base model, as well as daily minutes of vigorous physical activity (VPA) after log transformations.

	DM1 (n=20)		TDC (n=45)					
	Mean	SD	Mean	SD	*Adj Mean Diff	*95% CI of Adj Diff		*p-value
						Lower	Upper	
Tt.Ar (mm²)	193.3	43.3	208.4	41.0	**-27.1**	**-43.1**	**-11.2**	**0.001**
Tt.BMD (mg HA/cm³)	277.9	46.1	246.8	40.7	**30.0**	**8.2**	**51.9**	**0.008**
ln(Ct.Ar)	3.68	0.29	3.67	0.18	-0.04	-0.13	0.05	0.434
ln(Ct.TV)	5.88	0.29	5.87	0.18	-0.04	-0.13	0.05	0.434
ln(Ct.BV)	5.77	0.32	5.63	0.18	0.08	-0.02	0.17	0.117
Ct.BMD (mg HA/cm³)	771.0	62.8	690.5	52.4	**63.9**	**36.1**	**91.6**	**<0.001**
Ct.TMD (mg HA/cm³)	811.8	55.1	762.6	35.3	**33.9**	**13.8**	**54.0**	**0.001**
ln(Apparent Ct.Th)	-0.31	0.27	-0.54	0.17	**0.18**	**0.07**	**0.28**	**0.001**
ln(Fine Ct.Th)	-0.72	0.22	-0.96	0.14	**0.19**	**0.10**	**0.28**	**<0.001**
ln(Ct.Po)	-3.3	0.5	-2.6	0.3	**-0.53**	**-0.71**	**-0.34**	**<0.001**
Ct.Po.V (mm³)	14.3	8.4	23.0	11.8	**-7.6**	**-12.7**	**-2.5**	**0.004**
Ct.Po.Dm (µm)	143	7.1	162	9.9	**-18**	**-22.1**	**-13.5**	**<0.001**
Tb.Ar (mm²)	154.8	37.5	177.4	38.8	**-31.6**	**-48.4**	**-14.9**	**<0.001**
Tb.BMD (mg HA/cm³)	166.0	28.8	179.1	34.4	-7.0	-22.7	8.7	0.375
BV/TV (%)	13.8	2.4	14.9	2.9	-0.6	-1.9	0.7	0.374
Tb.N (1/mm)	2.1	0.2	2.3	0.2	**-0.1**	**-0.3**	**0.0**	**0.033**
Tb.Th (µm)	66	8.7	66	9.7	1	0.0	0.0	0.538
Tb.Sp (µm)	416	51.4	381	51.0	26	0.0	0.1	0.053
ln(Tb.Sp.SD)	-1.83	0.16	-1.94	0.21	0.07	-0.03	0.17	0.157

Abbreviations: Tt.Ar = total bone area, Tt.BMD = total bone mineral density, Ct.Ar = cortical area, Ct.TV = cortical total volume, Ct.BV = cortical bone volume, Ct.BMD = cortical bone mineral density, Ct.TMD = cortical tissue mineral density, Ct.Th = cortical thickness, Ct.Po = cortical porosity, Ct.Po.V = cortical pore volume, Ct.Po.Dm = cortical pore diameter, Tb.Ar = trabecular area, Tb.BMD = trabecular bone mineral density, BV/TV = trabecular bone volume fraction, Tb.N = trabecular number, Tb.Th = trabecular thickness, Tb.Sp = trabecular separation, Tb.Sp.SD = trabecular heterogeneity. *Bonferroni adjustment for multiple comparisons. †Covariates are evaluated as sex (girls=1, boys=2), years from age at PHV = -1.17y, forearm muscle area = 2327.4 mm^2, BMI z-score = 0.27, and ln(VPA) =2.72.
ln(x) = natural log transformation.